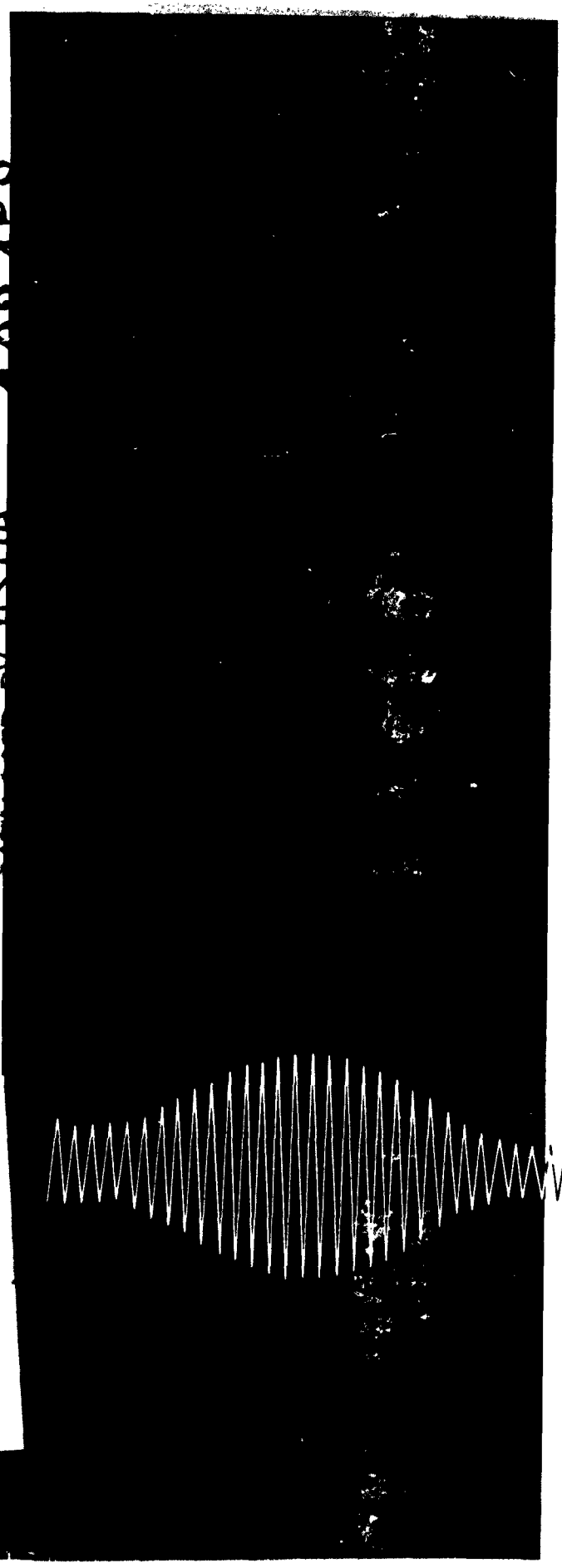

NANOSECOND PULSE BREAKDOWN STUDY

Final Report

Rome Air Development Center
Research and Technology Division
Air Force Systems Command
United States Air Force

Griffiss Air Force Base
New York

Contract No.
AF30(602)-2782

MICROWAVE ASSOCIATES, INC.

"Requests for additional copies by Agencies of the Department of Defense, their contractors, and other Government agencies should be directed to the:

ARMED SERVICES TECHNICAL INFORMATION AGENCY
ARLINGTON HALL STATION
ARLINGTON 12, VIRGINIA

Department of Defense contractors must be established for ASTIA services or have their 'need-to-know' certified by the cognizant military agency of their project or contract."

"All other persons and organizations should apply to the:

U. S. DEPARTMENT OF COMMERCE
OFFICE OF TECHNICAL SERVICES
WASHINGTON 25, D. C."

RADC-TDR-63-82 February 21, 1963

NANOSECOND PULSE BREAKDOWN STUDY

Prepared by:

C. Buntschuh

B. Salkins

Dr. M. Gilden

Approved by:

Dr. Grant E. St. John

MICROWAVE ASSOCIATES, INC.
Burlington, Massachusetts

Final Report

Contract No. AF30(602)-2782

Prepared
for
Rome Air Development Center
Research and Technology Division
Air Force Systems Command
United States Air Force

Griffiss Air Force Base
New York

FOREWORD

The objective of this contract was to explore the possibility of obtaining meaningful experimental data on microwave breakdown at pulse widths below twenty nanoseconds. The ultimate goal is super range resolution radar through the use of short pulses. The major problems of interest included application of breakdown theory to microwave nanosecond pulses to determine experimental requirements and provide a theory to compare with experiment, the design of a suitable experimental setup, and the design of components for the experimental setup.

Microwave Associates' approach followed the general outline of major problems stated in the last paragraph. Application of theory to the nanosecond case was accomplished insofar as this was possible. The experimental scheme is based on r.f. buildup and storage in a section of waveguide which is a few wavelengths in length. The naosecond pulse is formed when the waveguide section is quickly switched into another section of waveguide containing the test chamber. The most formidable problem is the waveguide switch, but progress on the development of a suitable switch has been encouraging to date.

Briefly, some of the more important conclusions are as follows:

(1) The theory predicts substantial increases in peak power handling capability for pulse widths below twenty nanoseconds even at the poorest pressures to be encountered in practical application.

(2) Further theoretical work is needed, especially as regards the effects of space charge, field distortion, differences in the breakdown mechanism at low and high pressures, gas heating, etc.

(3) The properties of high dielectric strength gases should be studied experimentally in the nanosecond region.

(4) Further improvement of the experimental scheme devised under this contract is desirable.

This contract is being extended for one year in order to accomplish the tasks outlined above.

WILLIAM C. QUINN
RADC Project Engineer

ABSTRACT

An estimate is made of the pulse breakdown characteristic for air on the basis of the theory worked out by Gould and Roberts[1] and the available data. The theory is critically examined and the consequences of the assumptions made are investigated to insure its applicability to extremely short pulse breakdown. Several possible modifications are advanced which require experimental verification with nanosecond pulse lengths. The possible advantages of using so-called high dielectric strength gas is also discussed. Progress on development of a nanosecond pulse generation circuit is reported; several ATR switches are described and discussed.

TABLE OF CONTENTS

LIST OF ILLUSTRATIONS

LIST OF TABLES

I. INTRODUCTION

How can one transmit very high peak power microwave signals through a waveguide system without being troubled by electrical breakdown of the gas filling the guide? There are various approaches to solving the problem, each with its own limitations of power handling ability and practicality. Specifically, one can:

a) evacuate the system

b) pressurize the system

c) fill the system with high-dielectric strength gas

d) transmit short pulses.

The work of this contract has been to examine the "short pulse" approach in detail in order to evaluate its promise.

The breakdown of a gas requires a certain length of time. For a given gas pressure this time becomes shorter as the applied electric field or transmitted power increases. Therefore, if the length of a microwave pulse is shorter than the breakdown time corresponding to its amplitude, the gas will not break down and the pulse will be transmitted undisturbed. Thus the problem becomes one of determining the breakdown field - pulse length characteristic of the gas filling the waveguide.

For significant increases in pulsed breakdown power levels over CW breakdown power at atmospheric pressure the time required is typically less than 10^{-7} or 10^{-8} sec. This fact brings up the second problem, that of producing high power pulses of such short duration.

Primary microwave sources to do this job are not available. A microwave circuit employing a resonant section of waveguide, which is charged by a long, relatively low power, magnetron pulse and discharged into the following waveguide section by means of a fast ATR-type switch, can yield the desired short pulses at higher peak power level than the magnetron can produce.

In this report an estimate is made of the pulse breakdown characteristic for air on the basis of the theory worked out by Gould and Roberts[1] and the available data. The theory is critically examined and the consequences of the assumptions made are investigated to insure its applicability to extremely short pulse breakdown. Several possible modifications are advanced which require experimental verification with nanosecond pulse lengths. The possible advantages of using so-called high dielectric strength gas is also discussed. Progress on development of a nanosecond pulse generation circuit is reported; several ATR switches are described and discussed. Further development of the fast switch and nanosecond pulse circuit is outlined. Some experiments to measure the nanosecond pulse breakdown characteristic, as well as additional experiments to study the basic breakdown mechanisms are suggested.

II. BREAKDOWN MECHANISM AND THEORY

An electric field applied to a gas initially containing some free electrons accelerates these electrons. Some acquire enough energy to ionize gas molecules and thereby create more free electrons, which, in turn, are accelerated and produce further ionization. An electron avalanche develops. Electrons are lost from the avalanche when they diffuse to the walls confining the gas or, in electronegative gases, when they attach to neutral molecules forming negative ions. The negative ions eventually recombine with positive ions and form two neutral molecules.

Electrical breakdown of the gas is governed by the relative rates of ionization and deionization. Denote the ionization rate per electron by ν_i (ionizations/sec-electron), the attachment rate by ν_a (attachments/sec-electron), the diffusion loss rate by ν_d (fractional losses/sec-electron) and the electron density by n (electrons/cm^3). The rate of increase of electron density is simply

$$\frac{dn}{dt} = \nu_{eff} n, \tag{1}$$

where $\nu_{eff} = \nu_i - \nu_a - \nu_d$ is the effective ionization rate per electron. If ν_{eff} is positive and constant, the density grows exponentially in time from an initial density n_o,

$$n = n_o e^{\nu_{eff} t}. \tag{2}$$

The rate of diffusion loss depends on the geometry of the container. For a differential volume element it is

$$\nu_d n = -D\nabla^2 n, \tag{3}$$

where D is the electron diffusion coefficient. With this term Eq. (1) becomes

$$\frac{\partial n}{\partial t} = (\nu_i - \nu_a)n + D\nabla^2 n. \tag{4}$$

The solution satisfying the boundary conditions, the electron density zero at the walls, is

$$n(\bar{r},t) = \sum_m n_m e^{(\nu_n - \frac{D}{\Lambda_m^2})t} X_m(\bar{r}) \tag{5}$$

where $\nu_n = \nu_i - \nu_a$ is called the net ionization rate, Λ_m is the diffusion length of the m^{th} diffusion mode and is determined by the geometry. $X_m(\bar{r})$ is a spatial function describing the electron

distribution associated with the m^{th} diffusion mode. The n_m are coefficients determining the amount of each mode present.

Infinite parallel plane electrodes separated by a distance d with a uniform gas density and uniform electric field is the simplest case. In this geometry $\Lambda_m = d/m\pi$ and $X_m = \cos x/\Lambda_m$, where $m = 1,3,5,7\cdots$ and x is the coordinate perpendicular to the electrodes as measured from the midplane between them. The lowest mode, $m = 1$, has the largest effective ionization rate and it is generally possible to neglect the higher modes. Then, we have

$$n = n(x,t) = n_1 e^{\left[\nu_n - D(\frac{\pi}{d})^2\right] t} \cos \frac{\pi x}{d} \qquad (6)$$

Hence, in Eq. (2) the initial density is $n_o = n_1 \cos \pi x/d$ and $\nu_{eff} = \nu_n - D(\pi/d)^2$. If $\nu_{eff} > 0$ for a pulse of length τ, the ratio of final to initial electron density is

$$\frac{n_f}{n_o} = e^{\nu_{eff}\tau}.$$

Taking logarithms, we obtain

$$\nu_{eff} = \frac{1}{\tau} \ln \frac{n_f}{n_o}$$

or

$$\nu_n = \frac{1}{\tau} \ln \frac{n_f}{n_o} + D\left(\frac{\pi}{d}\right)^2 \qquad (7)$$

Eq. (7) is the pulse breakdown relation used by Gould and Roberts[1] in which they set $n_f/n_o = 10^8$ or $\ln n_f/n_o = 18.4$ as giving best agreement with experiment.

The breakdown electric field is determined by Eq. (7) and the dependencies of ν_i, ν_a and D on the amplitude of the field E_o, its frequency and the gas pressure. The experimentally measured ionization parameter is the first Townsend ionization coefficient α, defined as the number of ionizations one electron makes in one centimeter drift along a dc electric field. Similarly, the empirical attachment coefficient η is the number of attachments per cm per electron. The electrons acquire a drift velocity v_d which is roughly proportional to the field. The constant of proportionality is the electron mobility μ, so that $v_d = \mu E$. The diffusion coefficient is $D = 2\mu\bar{u}/3$, where $\bar{u}$ is the average electron energy. A physcially important quantity is the amount of energy an electron acquires in a mean free path between collisions. Since the mean free path is inversely proportional to gas pressure, the energy gained per mean free path is proportional to the "reduced field" E/p volts/cm-mm Hg. The quantities α/p, η/p, v_d, μp, and $\bar{u}$ are all functions of E/p only and μp is essentially constant. They have been measured in dc electric

fields over limited ranges of E/p, as summarized in Table I. The net ionization rate is $\nu_n = (\alpha-\eta)v_d$, hence $\nu_n/p = (\alpha/p-\eta/p)v_d$ is a function of E/p only in a dc field

TABLE I

AVAILABLE DATA ON BREAKDOWN PARAMETERS FOR AIR

PARAMETER	RANGE OF E/p volts/cm-mmHg	REFERENCE
α/p	20-900	3, p 534; 4, pp 128,132
η/p	25-60	4, p 176
$v_d, \mu p$	0-22	4, p 58
$\bar{u}$	0.1-20	2
κ	0.1-20	2

All of the parameters depend on E/p by way of the electron energy $\bar{u}$. In an rf field of amplitude E_o and radian frequency ω the energy of the average electron is

$$\bar{u} = u_o \left[(1 + a \cos (2\omega t-\phi)\right] (1-e^{-\kappa\nu_c t}) \qquad (8)$$

where

$$\mu_o = \frac{e^2 E_o^2}{2\kappa m \nu_c^2 (1 + \frac{\omega^2}{\nu_c^2})} = \frac{e^2}{\kappa m (\frac{\nu_c}{p})^2} \left(\frac{E_e}{p}\right)^2$$

$$a = \sqrt{1/1 + \frac{4\omega^2}{\kappa^2 \nu_c^2}} \quad \text{(modulation factor)}$$

and

$$\phi = \tan^{-1} \frac{\omega}{\nu_c} .$$

The quantity κ is the energy loss parameter, that is the fraction of its energy an electron loses in a non-ionizing collision with a gas atom. The electron collision frequency ν_c is proportional to pressure, making ν_c/p a function of $\bar{u}$ or E/p. Both κ and ν_c/p depend upon E/p as shown by the data of Crompton, Huxley, and Sutton[2] in Fig. 1. The derivation of Eq. (8) assumes them to be constant. The measured $\bar{u}$(E/p) at dc is also given in Fig. 1. An rf field is less efficient than a dc field in heating the electrons and causing ionization. The actual rf amplitude must be multiplied by the frequency factor $1/\sqrt{2(1+\omega^2/\nu_c^2)}$ to obtain the equivalent dc field E_e. For air, Gould & Roberts use $\omega/\nu_c = 36/p\lambda$, where λ is the free space wavelength

of the microwave signal in cm. They took $\nu_c/p = 5.3 \times 10^9$ sec^{-1} mm Hg^{-1} which is higher than reported in Ref. 2, however we have continued to use that value for purposes of comparison. Gould and Roberts have accounted for energy modulation by averaging ν_n/p over an rf cycle and computing a correction curve from the $p\lambda = 0$ ($\omega/\nu_c = \infty$) limit. We shall therefore omit energy modulation effects and work with the infinite frequency limit as the reference breakdown curve.

The net ionization frequency is plotted in Fig. 2 as a function of E_e/p using the known α/p and η/p. The drift velocity is extrapolated to a value of $E/p = 900$ by the formula

$$v_d = (3.92 + .263\ E/p) \times 10^6 \text{ cm/sec},$$

which is approximately that used by Gould and Roberts[1]. The attachment coefficient becomes negligible for $E/p > 60$. The net ionization frequency was extrapolated to values of E/p between 900 and 1400 by eye where the upper limit is roughly equal to the collision frequency. Actually, at these extremely high values of E/p, ν_n/p has to decrease again, as the ionization efficiency decreases; the maximum will be broad and flat.

The data of Fig. 2 used in Eq. (7) yields the pulse breakdown curve of Fig. 3. Gould and Roberts show experimental points confirming this theory down to $p\tau = 1.7 \times 10^{-5}$ mm Hg-sec at which point $E_e/p = 53$ v/cm-mm Hg. The extreme point was at a pressure of 21 mm Hg

and pulse length of 0.8 μs, and $p\lambda$ = 275 mm Hg-cm. The un-normalized rms field strength was E_{rms} = 1110 v./cm, corresponding to about 27 kw peak pulse power in S band waveguide.

Except for E/p > 900, the limitations on the data used in the extrapolation are not serious. The extrapolation of the drift velocity over such a long range is questionable. If we use $v_d = (5 + .2\ E/p) \times 10^6$ cm/sec, obtained from the data in Ref. 4, a 60% smaller $p\tau$ is obtained at the higher values of E/p, which suggests that the extrapolation error is of the order of a factor of 2.

III. APPLICABILITY OF THEORY TO VERY SHORT PULSES

A. Discussion of the Theoretical Model

The breakdown relation, Eq. (7), is based on a model in which the following assumptions are made:

1. A uniform rf electric field is impressed on a gas at uniform pressure (molecular density) between infinite, parallel plane electrodes.
2. Higher mode diffusion is neglected so that the lowest mode (cosine density distribution) exists during most of the pulse. Regardless of the actual initial distribution, the cosine distribution is established so rapidly that it is considered to be the initial distribution.
3. Breakdown has occurred when the density increases by a factor of 10^8.
4. The net ionization frequency, diffusion coefficient, energy loss parameter, and collision frequency are all constant in space and time during the pulse, with values corresponding to the final electron energy $\bar{u}(E/p)$.
5. The electron heating transient is neglected.
6. Space charge effects are neglected.
7. The rf field is applied in a single, isolated pulse.
8. The ionization is by electron impact only (α process).

The question now is whether to expect this theory to remain substantially valid in the limit of very short pulses.

To neglect higher diffusion modes relative to the lowest requires first, that the decay time at the first higher mode be much shorter than the lowest. This is always true since the ratio of decay times for the first two modes between parallel planes is 1/9. Second, the pulse length must also be long compared to the higher mode decay time. These conditions will result in a cosine distribution and Eq. (7) applies. If the pulse is short enough to violate this assumption, any higher mode content, initially present, will reduce the rate of electron density growth so that Eq. (7) will predict a breakdown field which is too low. This is based upon the breakdown criterion $n_f/n_o = 10^8$ at the maximum in the distribution. An extreme limit of this situation, in which the electrons are initially localized in a plane parallel to the electrodes, is examined in Section B below. We shall see that this breakdown criterion, which results from fitting the theory to experiment, may lose significance when the initial electrons are highly localized and do not diffuse appreciably during the pulse.

To treat the breakdown parameters, especially the net ionization frequency as a constant in time, requires that the pulse length be long compared to the electron heating time, and that the parameters be averaged over a cycle when energy modulation is important. The validity of neglecting the electron heating transient, while taking into account the time variation of the energy loss parameter is analyzed in Section C and found to be justifiable in the short pulse limit.

The effect of space charge on the rate of growth of electron

density is not taken into account in this theory. Gould and Roberts determined breakdown by detecting the first occurrence of visible light with a phototube, it is possible that the density at this time in the development is not high enough to affect materially the transmission of a microwave signal, particularly if the ionized volume is still small. Space charge will inhibit the spatial growth of the ionized region and hence may be important in formulating a better breakdown criterion. Some theoretical work has been done on evaluating the space charge contribution to the breakdown time in dc fields[5,6] in which mobility loss and secondary emission of electrons are necessarily taken into account. These processes do not apply to rf breakdown. It was noted[6], however, that space charge begins to become important in air at atmospheric pressure at a current density of 10^{-5} amp/cm^2. This corresponds to an electron density of the order of 10^7 cm^{-3}, or an 8% impedance change at S band. More work, both theoretical and experimental are needed in this area, particularly applied to the microwave breakdown problem.

The problem of differences between low and high pressure breakdown has also received very little attention. The pressure scaling law E/p (pd, pλ, pτ) is generally assumed to hold at all pressures, whereas the experiments are usually performed at reduced pressure to keep breakdown power requirements down. Miller* has found both pulse length and pulse repetition rate dependence of breakdown power at atmospheric pressure with pulses 200 to 700 μs long which should be at the CW limit. Gould and Roberts augmented their theory to include

*Miller, S. J., Lincoln Laboratory, Private Communication.

repeated pulses by taking into account diffusion of electrons out of the gap between pulses. They checked this in the 25-300 mm Hg pressure range with a 0.8 μsec pulse and obtained general agreement. It is conjectured that a gas heating process occurs at sufficiently high pressure, in which the pulses may be far enough apart to be considered single and isolated as far as electron diffusion is concerned, but not for diffusion of heat in the gas. In this event, the below-breakdown electron cloud produced in one pulse will be almost all gone when the next pulse comes along. However, the energy the electrons acquire from the electric field is very rapidly transferred to the gas. This local heating of the gas will decrease its local molecular density, increasing E/p at that point. Thus the possibility exists for a series of pulses, relatively widely separated, to break the gas down at power levels less than pulse breakdown theory predicts. This heating phenomenon is also related possibly to the motion of a microwave arc in a waveguide[7].

There are several processes by which electrons are generated in a gap during breakdown. Free electrons may be produced from the gas atoms by electron impact or photo-ionization, or they may come from the walls by secondary, thermionic, field or photo electric emission. In general, at high pressures in rf fields any electrons emitted from the surface will not contribute significantly to the overall electron density or its growth rate. This source of electrons could be taken into account by changing the boundary condition on the solution to Eq. (4), to a non-zero value of electron density at the walls. This

would effectively increase the diffusion length of the gap slightly. Thus, when the pressure is high enough that the breakdown field is independent of pd, it will also be unaffected by any surface emission of electrons. Photo ionization and streamer formation are generally important on extremely non-uniform fields[9], and is probably negligible in other cases. It is therefore reasonable to assume that the impact ionization process is the only significant one operating in rf breakdown when diffusion is negligible, i.e., at high pd or short pulse length.

B. Electron Diffusion

A breakdown avalanche may be initiated by a single electron, or perhaps a localized group of electrons such as might exist after passage of a cosmic ray. If the pulse is short compared to the diffusion time τ_D, $p\tau_D \approx 10^{-6}(pd)^2$ mm Hg-sec electrons will scarcely diffuse at all and the entire avalanche may be fairly localized in space. The breakdown field predicted by Eq. (7) would appear low in that the breakdown would be incomplete and the ionized region would not fill an appreciable portion of the gap. On the other hand, the field strength is sufficient to increase the central density by 8 orders of magnitude.

Let us then assume a uniform initial electron density n_1 in a thin layer δ which is diffusing into adjacent regions in the presence of a uniform rf electric field. The walls may be considered infinitely remote. The density distribution n(x,t) will proceed as sketched in Fig. 4a. The analytic solution, obtained by standard Fourier Integal technique*, is

*Hildebrand, C. F., Advanced Calculus for Engineers, Prentice-Hall 1949 p. 455.

$$n(x,t) = \frac{n_i}{2} e^{\nu_n t}\left[\operatorname{erf}\left(\frac{x+\frac{\delta}{2}}{\sqrt{4Dt}}\right) - \operatorname{erf}\left(\frac{x-\frac{\delta}{2}}{\sqrt{4Dt}}\right)\right],$$

which reduces to

$$n(x,t) = n_i \delta\, e^{\nu_n t}\, \frac{e^{-x^2/fDt}}{\sqrt{4\pi Dt}} \qquad (9)$$

as $n_i \to \infty$ and $\delta \to 0$ but $n_i \delta$ remains finite. The temporal growth at $x = 0$ given by Eq. (9) is compared with that of Eq. (6) in Fig. 4b. Note that the volume density initially drops from infinity to a minimum in a time $t_{min} = 1/2\ \nu_n$, i.e., one half the time it takes the electron density to increase by a factor of e. We have taken this minimum value to be n_o, the initial central density of the lowest diffusion mode case, i.e., Eq. (7) becomes

$$n(x,t) = \frac{n_o}{\sqrt{2e\nu_n t}}\, e^{\nu_n t}\, e^{-x^2/4Dt}\ .$$

Fig. 4b covers just 5 time constants, while 18.4 may be required for breakdown. Clearly the difference in the curves within the first time constant is of no real consequence on the breakdown time scale.

The width of the ionized region grows with the square root of

time, which is slow compared to the exponential growth in density. The width at "half-height" is $x_{1/2} = \sqrt{4(\ln 2)Dt}$. At one atmosphere this is approximately $x_{1/2} \approx \sqrt{t/25}$ cm, with t in microseconds. Even for pulses of 1 μsec this is very small spreading.

If we adapt the $n_f/n_o = 10^8$ breakdown criterion to the present problem, calling the density at $t = t_{min}$ the equivalent initial density, we can write the breakdown relation as

$$\frac{\nu_n}{p} = \frac{21}{p\tau} \tag{10}$$

The relation of Eq. (7) for infinite gap width is

$$\frac{\nu_n}{p} = \frac{1}{p\tau} \ln 10^8 = \frac{18.4}{p\tau} \tag{11}$$

Eq. (10) yields a 14% higher ν_n/p and at $p\tau = 10^{-8}$ a 5% higher breakdown E/p than Eq. (11). The data and the extrapolated breakdown curve of Fig. 3 are centainly not good to 5%. This leaves little logical basis for choosing either initial condition in preference to the other using the $n/n_o = 10^8$ breakdown criterion. However, for short pulses there is no need to retain this criterion; a more useful breakdown criterion might be based on the impedance perturbation of the ionized volume in the waveguide.

This analysis has neglected the electron drift motion in the electric field, space charge and field distortion. These effects should be examined. They may help to explain the filamentary arc type of breakdown encountered at pressures greater than a few cm-Hg.

C. Electron Heating Transient

The rate of electron heating is determined by the rate of energy gained from the electric field and the rate of energy lost in collisions with atoms. It is given by

$$\frac{du}{dt} = P - \kappa \nu_c u \tag{12}$$

where u is the energy of the average electron, $\kappa(u)$ is the energy loss parameter (Fig. 5), $\nu_c(u)$ is the collision frequency and $P = (e^2 E_e^2/m\nu_c)\left[1 + a \cos(2\omega t + \phi\right]$ is the power input to the electron from the field. For zero initial energy and constant $\kappa\nu_c$, the heating transient is given by

$$u(t) = \frac{P}{\kappa\nu_c}\left(1-e^{-\kappa\nu_c t}\right) \tag{13}$$

The final energy is $u_\infty = P/\kappa\nu_c \sim (E_e/p)^2$ and the heating time constant is $\tau_h = 1/\kappa\nu_c$.

The approximation of $\kappa(u)$ sketched in Fig. 5, which allows Eq. (12) to be solved in closed form, was used. The result is compared

with the constant $\kappa = \kappa(u_\infty)$ solution in Fig. 6. Note that both time constants are essentially the same, but that the non-constant $\kappa(u)$ case attains 90% of u_∞ in one τ_h, whereas it is only 63% when κ is constant. In both cases the heating time scales with pressure such that $p\tau_h$ is a function of E/p. This is plotted for in Fig. 7 and on Fig. 3. It is readily seen that at any E/p, the heating time is indeed negligible compared with the pulse length required for breakdown.

IV. HIGH DIELECTRIC STRENGTH GASES

The dielectric strength of a gas may be defined as its dc sparking potential relative to nitrogen at a pd large enough to make diffusion losses negligible. A few high-dielectric strength gases and their strengths measured at dc conditions at pd = 50 cm-mm Hg are[10]

N_2	1.00
$CHClF_2$ (Freon-22)	1.17
SF_6	1.82
$CHCl_2F$ (Freon-21)	1.82
CCl_2F_2 (Freon-12)	2.02
C_4F_8 (Freon-C-318)	2.44
$CClF_2$-$CClF_2$ (Freon-114)	2.97
$CHCl_3$	3.01
CCl_4 (low vapor pressure)	3.2

At microwave frequencies the equivalent ratios for SF_6, Freon 12, Freon 114 and Freon C318 have been found to be considerably larger[11]. These gases are electronegative, and rely principally on high values of attachment coefficients and, perhaps to a lesser extent, on low values of Twonsend coefficients for their high sparking potentials. The breakdown field is determined by that value of E/p for which the net ionization frequency is zero, i.e., the ionization frequency equals the attachment frequency. In general the ionization frequency increases

much more rapidly than the attachment frequency as E/p increases. Thus, at the higher E/p values required for pulse breakdown, attachment losses may become negligible and only the relation between ionization rate or the Townsend coefficient and E/p determines the breakdown field.

The available data on the Townsend coefficient α/p for the high dielectric strength gases is sparse, covers small ranges in E/p and is probably unreliable because of the difficulty of accurately measuring α in attaching gases. Data on attachment coefficients η/p are practically non-existent. However one can make some rough comparison of gases by extrapolating what data is available.

The theory of the Townsend coefficient[3] yields the semi-empirical formula

$$\frac{\alpha}{p} = Ae^{-Bp/E} \qquad (14)$$

B and B/A are called the Stoletow constants of the gas. If $\ln\alpha/p$ is plotted versus p/E a straight line of slope - B should result. For any simple, non-attaching molecular gases this law is obeyed over a wide range of E/p. It generally fails for monatomic gases. There is not enough data on the complex electronegative gases to know how well it works. Considerable work has been done on the complex hydrocarbons (non-attaching) by Heylen and Lewis[18], and Devins and Crowe[18]. These workers have measured the A and B coefficients for

numerous hydrocarbons over respectable ranges of E/p and find the law valid at least up to E/p ~ 200 v/cm-mm Hg.

The log α/p for several gases is plotted against p/E in Fig. 8. All the curves are transcribed from Ref. 3 except the SF_6 curves labeled HG and WSB. The HG is from Birks and Hart[13] attributed to Harrison and Geballe. The WSB is determined from breakdown data published by Wilson, Simmons, and Brice[15]. The diversity in the SF_6 data points out the need for more basic data in this area. The A and B coefficients from these curves are roughly:

	B	A
N_2	320	14
CCl_2F_2	350	22
CH_5Cl	384	410
CF_3CF_5	635	61
C_2H_5Br	933	7×10^9
C_5H_{12}	1380	3×10^{11}
SF_6(v.Engel)	1920	3×10^{11}
$CHCl_3$	2880	6×10^{12}
CCl_4	7670	10^{21}

It is virtually certain that gases with anomalously high values of A either do not follow this law, or α/p was inaccurately measured.

Despite all the difficulties in estimating α/p for very high E/p in the high dielectric strength gases, a most striking feature emerges. All α/p tend to approach or cross that of air at high E/p. For $E/p \gtrsim 200$ it would seem that the advantage over air of the high

strength electronegative gases is considerably diminished, or lost altogether. The validity of this speculation depends of course upon the behavior of the attachment coefficient at high E/p. The attachment coefficient for Freon 12 was measured by Harrison and Geballe and is given in Ref. 3. It has a maximum of about 1 attachment/cm-mm Hg at E/p = 110 v/cm-mm Hg. It has not been measured for the other gases; attempts have been made to measure attachment cross-sections in SF_6 but numerical values are still controversial. There is still much difficult work to be done in this field. Nevertheless, it is probably safe to say that η/p becomes negligible compared to α/p for E/p greater than a few hundred in all cases.

V. NANOSECOND PULSE GENERATION CIRCUIT

The basic microwave circuit for generating very short, high power pulses are shown schematically in Fig. 9. Its principle of operation is as follows. A long, low-power microwave pulse from the primary source (magnetron) is coupled into a resonant cavity through a coupling iris. The cavity consists of a straight section of waveguide, coupling iris at the input end, and an ATR switch at the output end. The ATR switch ideally presents a series open circuit in the transmission line. The standing wave in the cavity has a voltage minimum at the input iris and a voltage maximum at the output open circuit; its amplitude is determined by the dissipative and coupling losses of the cavity. At some time during the input pulse, after the cavity is charged up, the ATR switch is fired. Then the forward traveling component of the standing wave moves toward the load; the backward traveling component reflects off the input iris and joins onto the forward going wave, and a pulse of twice the electrical length of the cavity travels toward the load. The pulse rise time is determined by the speed with which the switch closes.

To get the most out of this circuit, the cavity must be designed for optimum power gain and the ATR switch for high speed and low loss. The cavity design is straightforward, however, the design of a good nanosecond microwave switch is a major problem. In Section B several switches which were tried are discussed and two lines of attack for further experimentation are considered.

A. Cavity Resonator Circuit Analysis

A transmission line diagram of the cavity at resonance is shown in Fig. 10. The unfired ATR switch is a shorted stub in the E-plane. The short is 1/4 wavelength from the cavity waveguide wall, where it appears as an open circuit. The switch conductance, g, allows for losses in the switch and the fact that it is not a perfect open circuit, permitting some power to leak through to the matched load. The coupling iris is represented by a susceptance, b across the line. The power gain of the resonator is defined as the ratio of the power carried by the forward traveling component of the standing wave, just inside the iris, to the power carried by the incident wave. The square root of the power gain at resonance is the voltage gain and is given by

$$G_V = \frac{b}{a_1} = \frac{C}{1-L\sqrt{1-C^2}} , \qquad (15)$$

where $C = 2/\sqrt{4+b^2}$ is the coupling coefficient of the iris and $L = (1/1 + 2g)e^{-2\alpha\ell}$ is the attenuation suffered by the wave in making one round trip in the cavity. The waveguide attenuation constant is α, the cavity length ℓ. For resonance the electrical length must be

$$\theta = \frac{2\pi\ell}{\lambda g} = \left[(n-\tfrac{1}{2})\pi - \tfrac{1}{2}\tan^{-1}\frac{2}{b}\right] \qquad (16)$$

where n = 1, 2, 3···. Maximum gain is obtained when the input susceptance is adjusted for critical coupling, that is when

$$\sqrt{1-C^2} = \frac{b}{\sqrt{4+b^2}} = L \ . \qquad (17)$$

The power gain is plotted against the coupling for various loss factors L, in percent, in Fig. 11. This, in conjunction with Fig. 12, can be used to convert standing wave measurements in the input line to power gain once the loss is known. The loss can be determined by measuring the cavity Q.

The overall power gain is the ratio of the power at the output, after the switch is fired, to the input power. If the fired switch were lossless the overall gain would be just the cavity gain as plotted in Fig. 11 times the one-way waveguide attenuation $e^{-\alpha \ell}$.

B. Switch Design and Results

An effective ATR switch for the nanosecond pulse generation circuit must

a) be a good open circuit in the unfired state,

b) be a good short circuit in the fired state,

c) have a switching time of the order of a nanosecond,

d) be capable of holding off about one megawatt of rf power.

It should also not seriously reduce the waveguide bandwidth when fired, nor should it fire randomly or erratically. Of the various switching media used at microwave frequencies, a gas discharge switch

appears to be best able to meet the above requirements.

Five different switch designs with various modifications were tried. They are schematically illustrated in Fig. 13. The arm of an E-plane tee, Fig. 13a, which joins the broad wall of the cavity waveguide contains the switch element and is terminated by a movable short. The short is placed so as to appear as an open circuit in the cavity wall when the switch is not fired. The gas discharge switch is placed in the junction in the plane of the cavity wall, or a half wavelength back, so as to create a short circuit at the wall when fired. There is some sacrifice in bandwidth when the switch is a half wavelength from the junction because the electrical length to the short varies with frequency.

The two simplest switches, Figs. 13b d, consisted of a capacitive post and slot, respectively, across the junction, leaving narrow gaps. These gaps were broken down by the cavity power after triggering with ultraviolet light from an external spark gap. Another design, Fig. 13c, replaced the capacitive bar with a split post containing the trigger spark gap. This put the trigger source much closer to the main gap and offered some improvement. The switch of Fig. 13c, had a quartz tube, filled with air at approximately 200 mm Hg, situated immediately behind a resonant slot. A high voltage trigger pulse was applied across the electrodes to break the gas down and the rf power maintained the discharge. Another switch, Fig. 13f, consisted of two hemispheres mounted on opposite broad walls of the tee, with a .040" gap, located a half wavelength from the junction. It was triggered either by a

pointed electrode passing through the narrow wall to the gap center, or by light from an external spark gap.

All switches tried worked; but not well enough for the contemplated breakdown studies. They were satisfactory open circuits in the unfired state with typically 35 db isolation of the cavity from the load; but in the fired state the effective short circuit was inadequate. This is a consequence of the rf power in the cavity being unable to maintain a sufficiently dense discharge. Two important factors are the volume of the region being ionized and the equivalent impedance of the resonant structure through which the discharge is being initiated. Thus, the switching volume should be as small as possible and the equivalent impedance as low as is consistent with the desired power gain. The switches were evaluated with a sampling oscilloscope and the trigger was provided by a high voltage pulser which fired an auxiliary gap.

The low pressure switch had the best operating characteristics; it was a better short and fired more regularly than the others. However, because of the low pressure the switch operated slowly and could only hold off 400 kw of cavity power in standard WR90 waveguide. Pulses obtained using this switch had a 15 ns rise time and were about 80 ns long. The high pressure switches operated more rapidly; however the instrumentation was not adequate for accurate measurements.

To make a switch which produces a better short circuit, it will probably be advantageous to rely on an external source of power to maintain the discharge. To get fast switching, a high pressure discharge

using the geometry of Fig. 13e and external power should be tried. This type may produce a rounded leading edge to the pulse and require some pulse sharpening compensation, but it should be easier to minimize jitter[16]. An alternative scheme which should also be tried is the low pressure, or "vacuum" switch[17]. The discharge in this type is in the metallic vapor evaporated from the electrodes. A fairly long delay, of the order of 100 ns, is required before the initial weak discharge reaches the point where metallic vapor appears; from then on the dense switching plasma forms rapidly. This long delay could be desirable if it eliminates the need for a delayed trigger pulse and can be triggered simultaneously with the magnetron pulse. Again an auxiliary dc power supply is needed, but the switching time is less sensitive to voltage fluctuations than the high pressure type.

A typical pulse envelope is sketched in Fig. 14. The dotted curve represents the magnetron pulse, the solid curve the power into the load or detector. When the magnetron comes on, a small amount of power leaks through to the load before the switch fires. The trigger pulse closes the switch and the high power nanosecond pulse travels down the line, its amplitude distorted by arc loss and any other imperfections in the switch operation. Once the pulse has gone by the switch slowly recovers, reducing the output power gradually. Since there is still some power in the line, the switch may not recover fully until the magnetron pulse ends.

VI. SUGGESTED EXPERIMENTAL PROGRAM

It has been pointed out in Sections II and III that an experimental determination of the pulse breakdown characteristic for air for $p\tau < 10^{-5}$ mm Hg-sec is necessary for reliable estimates of the power handling capacity of pulsed microwave systems. Because of the possible differences between low and high pressure breakdown mechanisms, the experiments ought to be done as close to one atmosphere as possible. This requires pulses of the order of 10^{-8} sec. Video pulses could be used, but the correspondence to microwave breakdown is not assured, since electrons drift in the electric field to the walls (mobility-controlled breakdown) and secondary electrons may be emitted from the walls by ion impact. These contributions to the breakdown mechanism may become significant in the narrow gaps which are usually required to produce high fields at reasonable voltages.

Microwave pulse breakdown measurements yield useful information on the Townsend coefficient and can be used to study other gases at high E/p.

If more details on the breakdown mechanism are known, it may be possible to devise methods to suppress breakdown to a greater extent. Therefore, it would be desirable to know a) where the electrons come from and how the spark starts, b) how it grows in space and time, c) how large it must be before interferring with transmission, and d) how the pulse repetition rate influences breakdown by residual electrons and gas heating.

A minimum experimental program would include: a) development of the nanosecond pulse circuit for reliable, repeatable pulses down to 10 ns duration, b) design and construction of the breakdown chamber, c) measurement of breakdown characteristic of air to smallest possible $p\tau$, varying p and τ independently. The basic circuit arrangment is sketched in Fig. 14.

A more ambitious program would include: a) similar pulse breakdown measurements on high dielectric strength gases, in particular SF_6 and the Freons, b) experiments to measure temporal and spatial growth of the spark - probably a major undertaking, and c) experiments to determine the effect and importance of gas heating and the pulse repetition rate on lowering of breakdown fields.

VII. CONCLUSIONS

The pulse breakdown curve for air indicates that at atmospheric pressure the peak power for breakdown with a 10 ns pulse is approximately four times the CW power; with a 1 ns pulse it is about fourteen times the CW power. Modest gains in waveguide and antenna power handling capability are possible at atmospheric pressure using the nanosecond pulse technique. At reduced pressure enormous gains are possible; with a pulse with a $p\tau \approx 5 \times 10^{-8}$ mm Hg-sec one hundred times the CW power, at the same pressure, can be transmitted. There is also some hope of improving on this theoretical estimate by a better understanding of the breakdown mechanism and searching for ways of suppressing spark formation. Presently, in practice, the theoretical minimum breakdown powers are often not even attained, perhaps due to gas heating, surface irregularities or other effects.

In order to understand better the breakdown process, especially for very short pulses, more theoretical work is needed. The problems of space charge and field distortion, differences in the breakdown mechanism at low and high pressures, gas heating, and mode of spark propagation need particular attention. Experimental work to verify the theory is clearly required; a determination of the breakdown field pulse-length characteristic should be the essential goal of the experimental program. The properties of high dielectric strength gases are not well known and they should certainly be measured to determine the efficiency of the gases in the nanosecond pulse region.

REFERENCES

1. Gould, Roberts, J.A.P. 27, 1162 (1956)
2. Crompton, Huxley, Sutton, Proc. Roy. Soc. A218, 507 (1953)
3. von Engel, Handbuch der Physik XXI, pp. 530, 540
4. Brown, Basic Data of Plasma Physics
5. Ward, Fifth Inter. Conf. on Ionization Phenomena in Gases, Munich 1961
6. Miyoshi, Phys. Rev. 117, 355 (1960)
7. Gilden, "Ultra High Power Transmission Line Techniques", Second Technical Note (AF30(602)-2545), 19 June 1962
8. Brown, Handbuch der Physik XXII, p 539
9. Loeb, Basic Processes of Gaseous Electronics, U. Calif. Press, Berkeley, 1960
10. Birks, Schulman, eds. Progress in Dielectrics, Wiley & Sons 1959 p 150
11. Gilden, "High Power Capabilities of Waveguide Systems", Quarterly Reports, NObsr 85190, April 1961 - July 1962
12. Heylen, Lewis, Cam. Journ. Physics 36, 712 (1958)
13. Deuins, Crowe, Journal Chem. Physics 25, 1053 (1956)
14. Birks, Hart eds, Progress in Dielectrics, Academic Press, 1962, p 159
15. Wilson, Simmons, Brice, J. App. Phys. 21, 203 (1950)
16. Fletcher, Rev. Sci. Inst. 20, 861 (1949)
17. Hancox, Rev. Sci. Inst. 33, 1239 (1962)

FIGURE 1a
ELECTRON ENERGY LOSS PARAMETER FOR AIR
FROM REF. 2

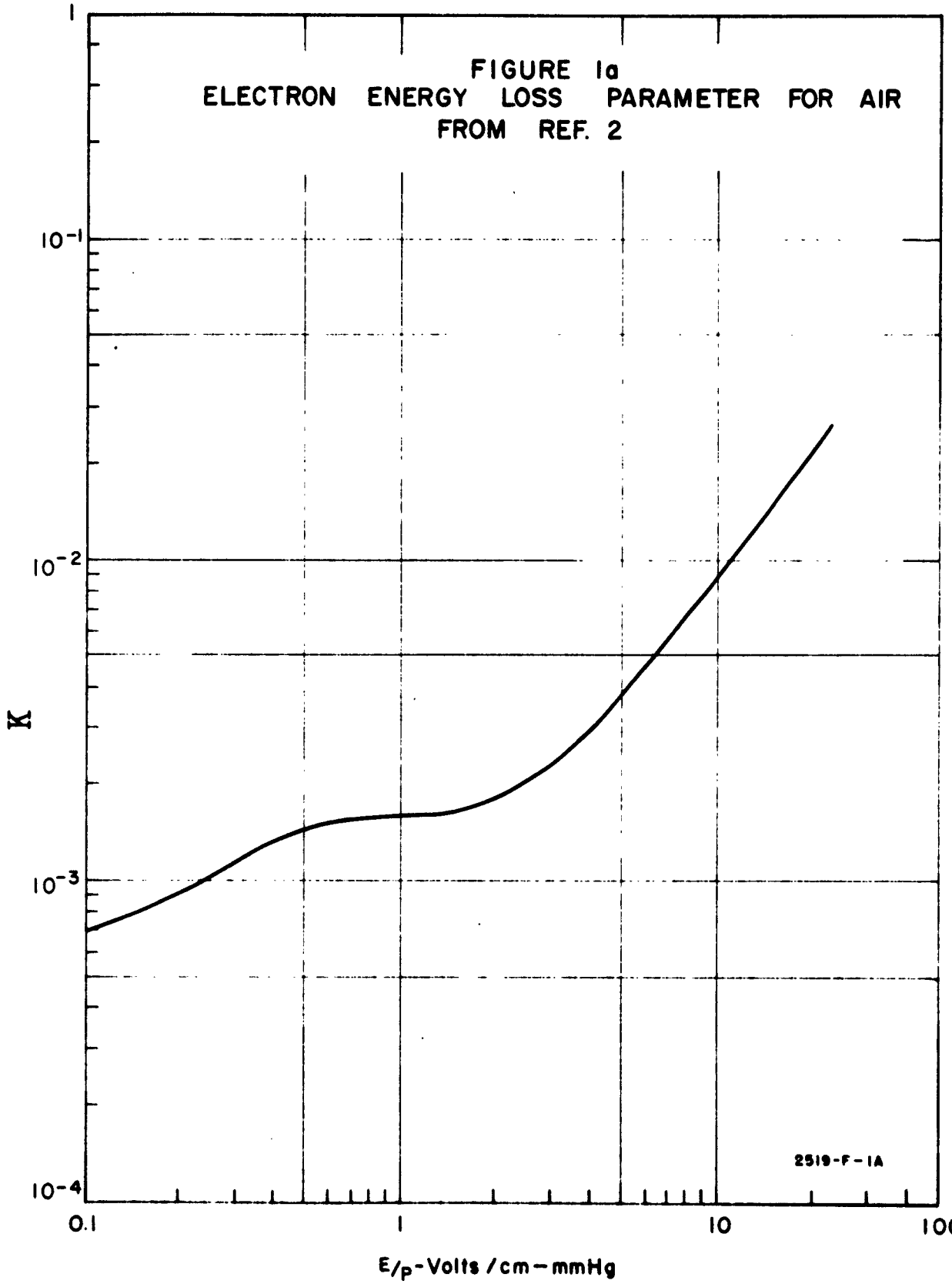

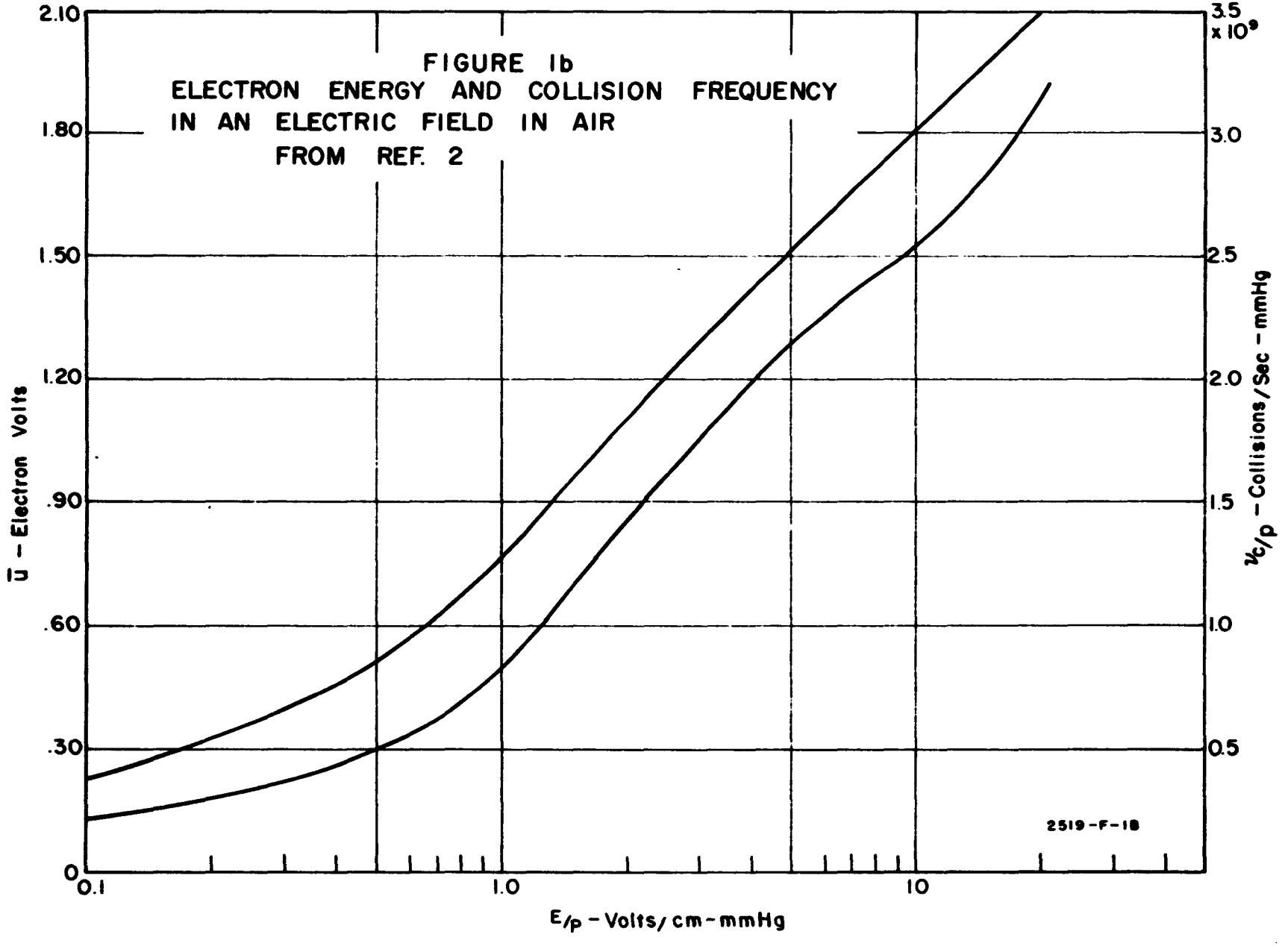
FIGURE 1b
ELECTRON ENERGY AND COLLISION FREQUENCY
IN AN ELECTRIC FIELD IN AIR
FROM REF. 2
2.10
1.80
1.50
1.20
.90
.60
.30
0
3.5
x 10⁹
3.0
2.5
2.0
1.5
1.0
0.5
0.1
1.0
10
ū - Electron Volts
νc/p - Collisions/Sec - mmHg
E/p - Volts/cm - mmHg
2519-F-18

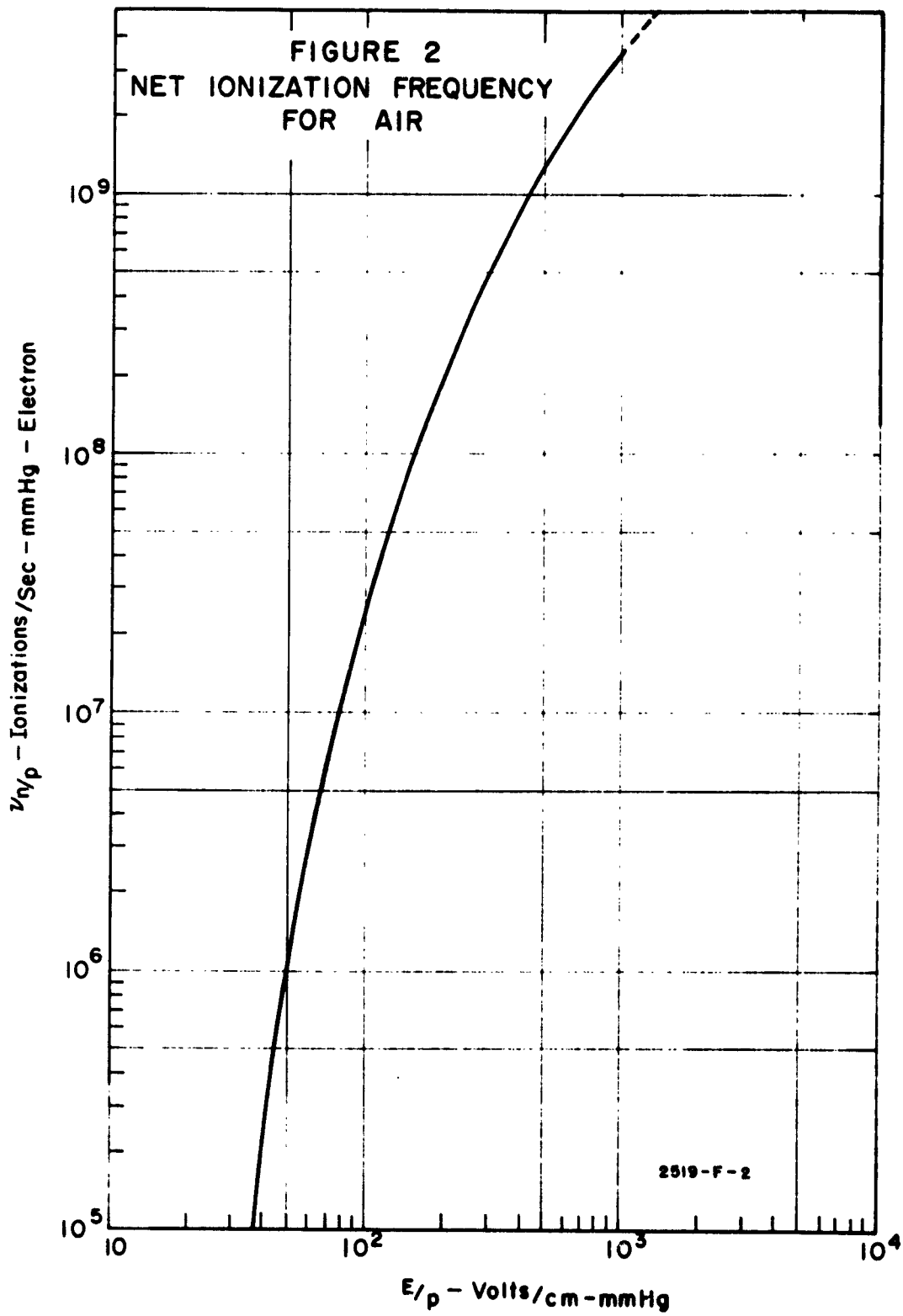
FIGURE 2
NET IONIZATION FREQUENCY
FOR AIR
10^9
10^8
10^7
10^6
10^5
$\nu_{\eta/p}$ – Ionizations/Sec – mmHg – Electron
10
10^2
10^3
10^4
E/p – Volts/cm – mmHg
2519-F-2

FIGURE 3

EXTRAPOLATION OF PULSE-BREAKDOWN CURVE TO LARGE VALUES OF E/P

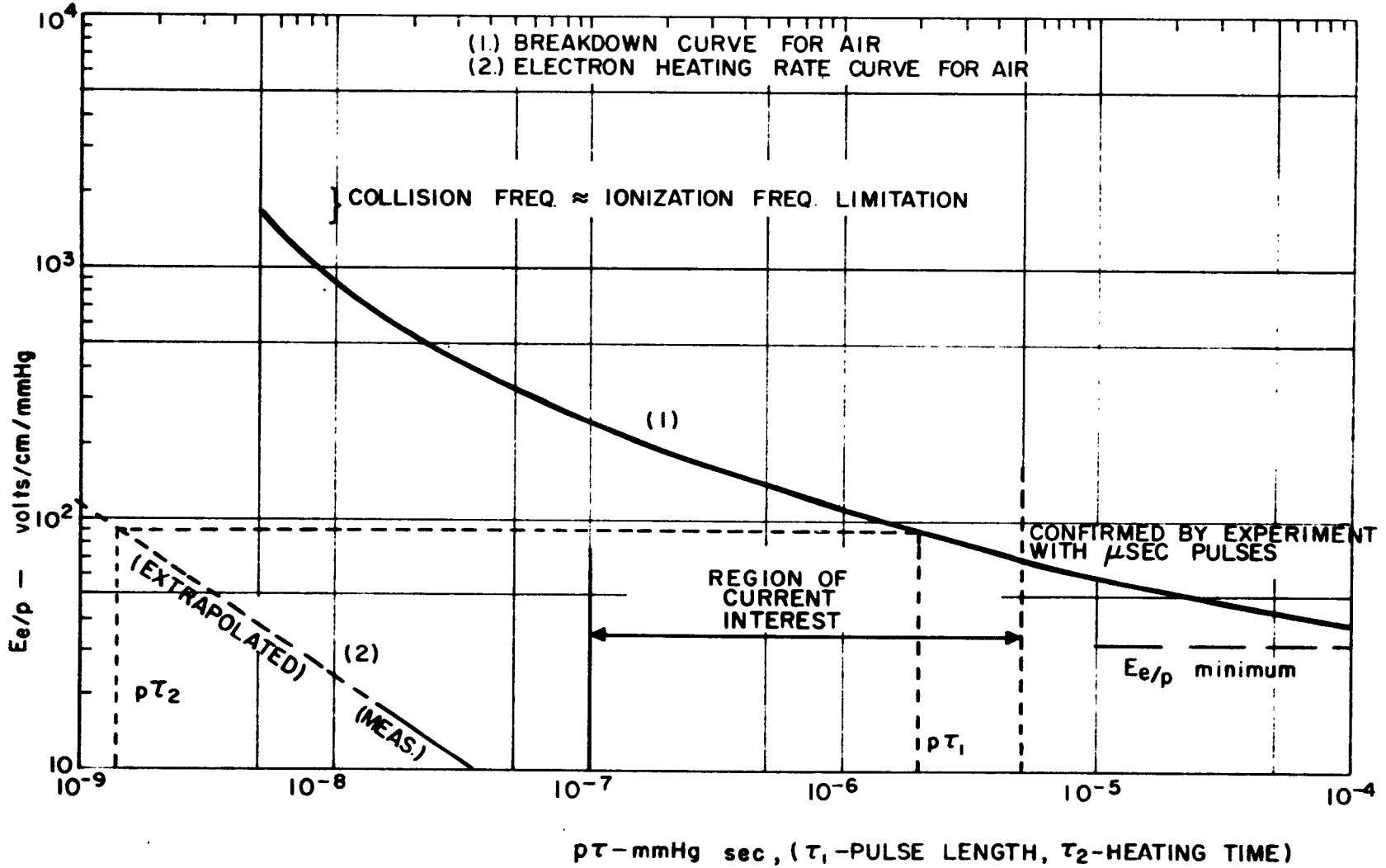

2519-F-3

FIGURE 4
GROWTH OF ELECTRON DENSITY

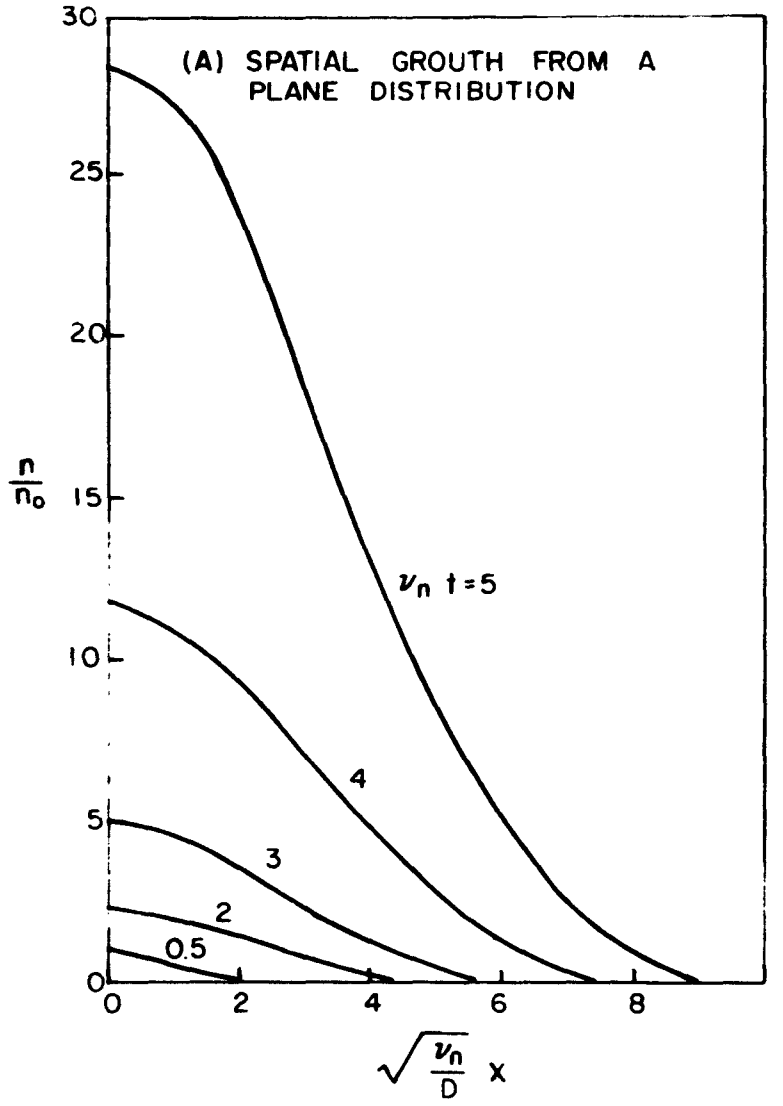

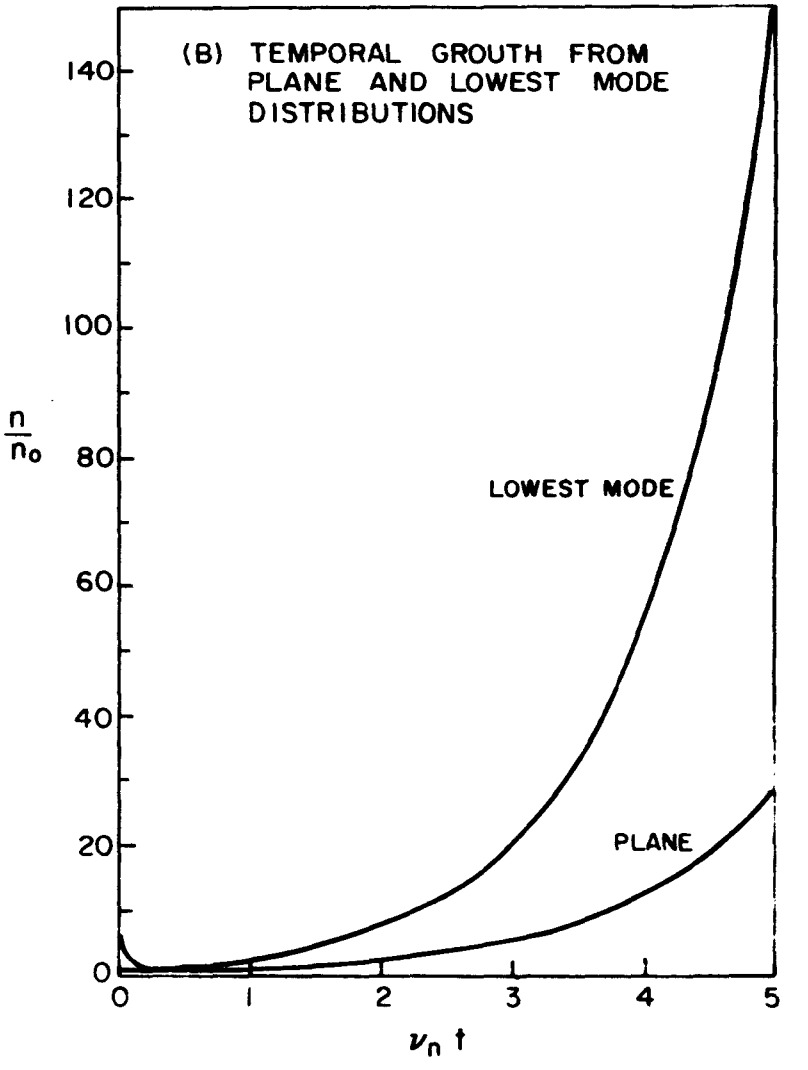

2519-F-4

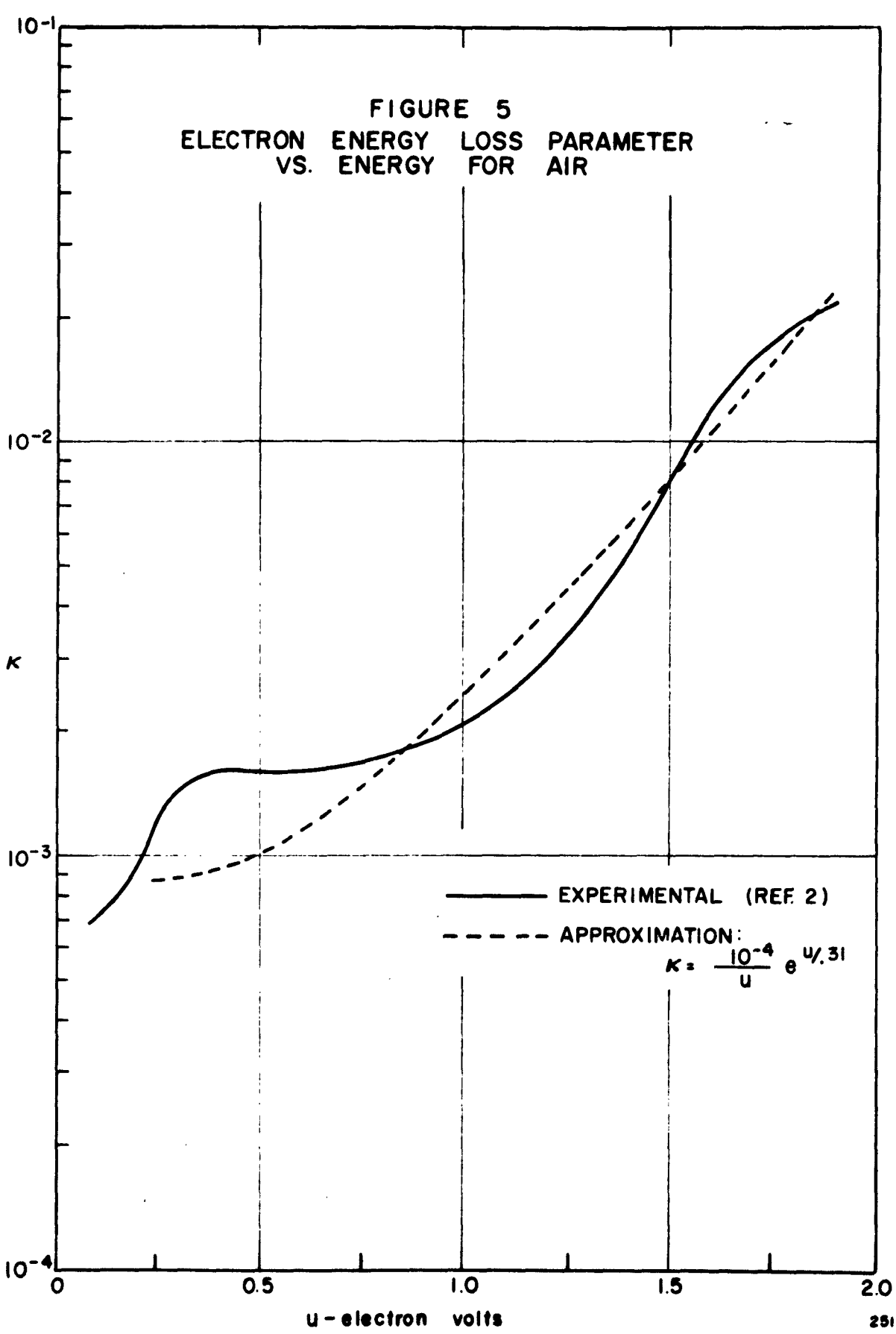
FIGURE 5
ELECTRON ENERGY LOSS PARAMETER
VS. ENERGY FOR AIR
10⁻¹
10⁻²
10⁻³
10⁻⁴
K
0
0.5
1.0
1.5
2.0
u - electron volts
EXPERIMENTAL (REF. 2)
APPROXIMATION:
K = 10⁻⁴/u e^(u/.31)
2519-F-5

FIGURE 6
ELECTRON HEATING TRANSIENT
IN AIR

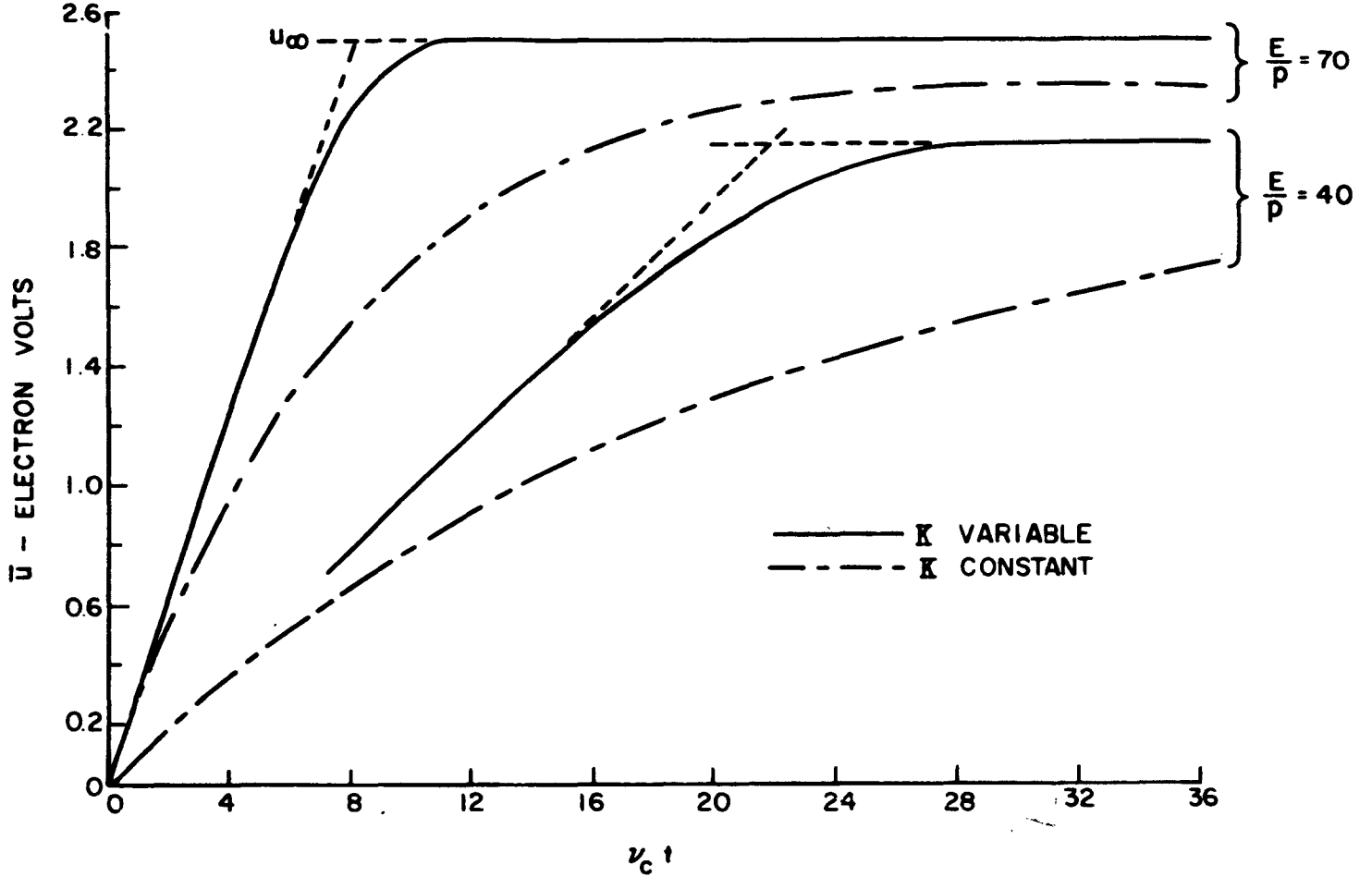

2519-F-6

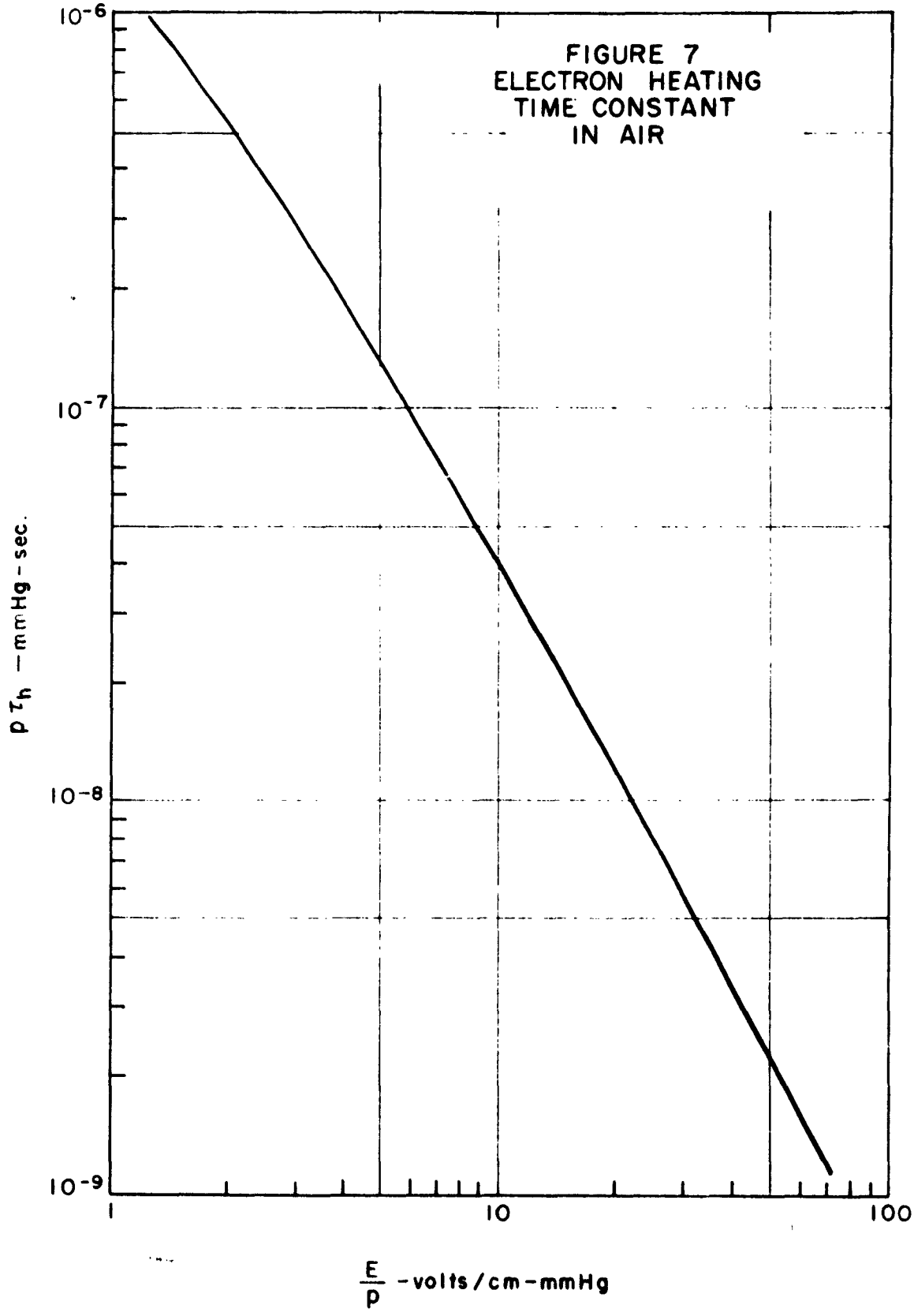
FIGURE 7
ELECTRON HEATING
TIME CONSTANT
IN AIR
10^{-6}
10^{-7}
10^{-8}
10^{-9}
$p\tau_h$ – mm Hg – sec.
1
10
100
$\frac{E}{p}$ – volts / cm – mm Hg
2519-F-7

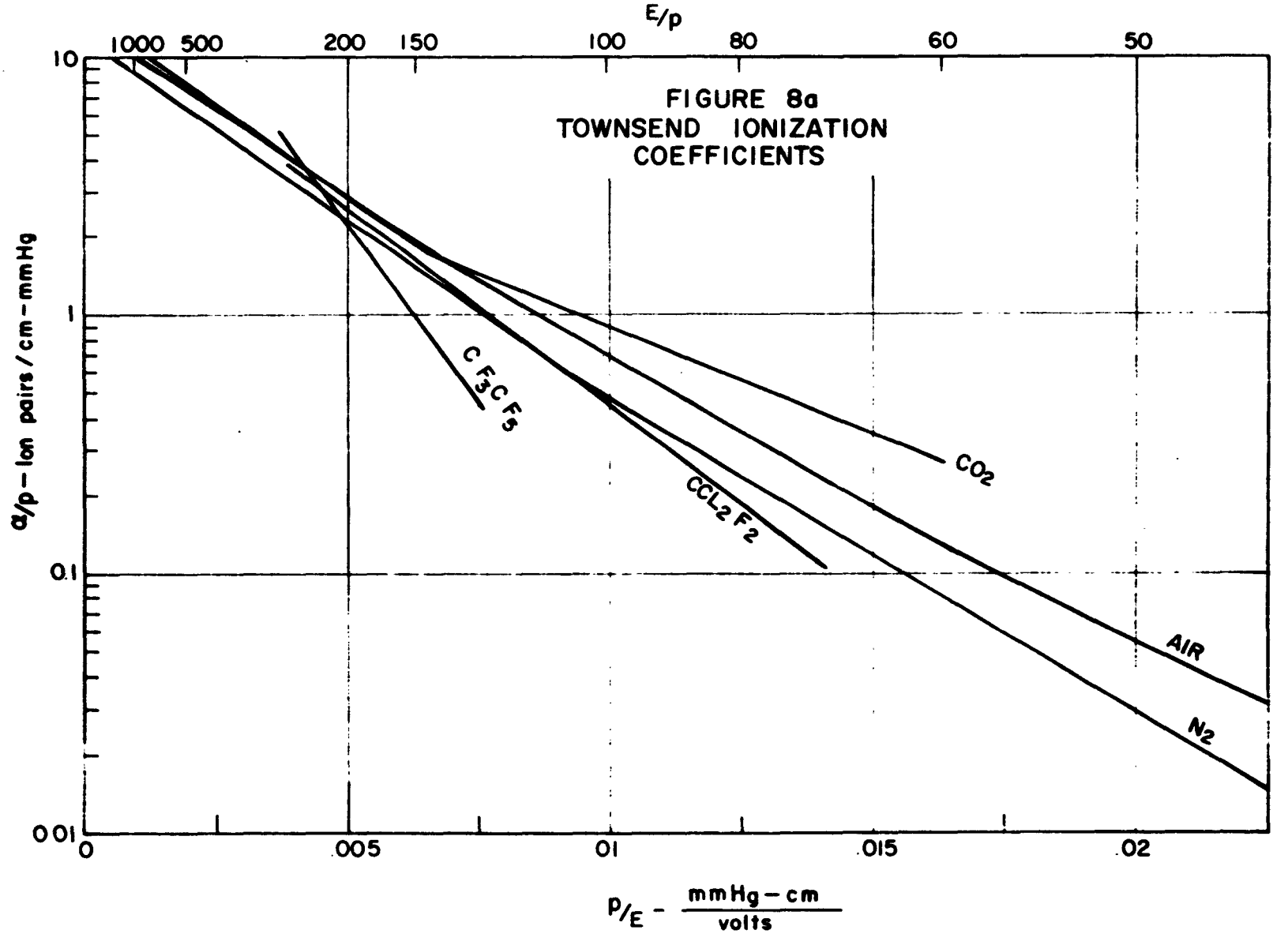
E/p
1000
500
200
150
100
80
60
50
10
1
0.1
0.01
α/p – Ion pairs / cm – mm Hg
FIGURE 8a
TOWNSEND IONIZATION
COEFFICIENTS
$C_2F_5C_F_3$
CO_2
CCL_2F_2
AIR
N_2
0
.005
.01
.015
.02
p/E - $\frac{mm\,Hg - cm}{volts}$

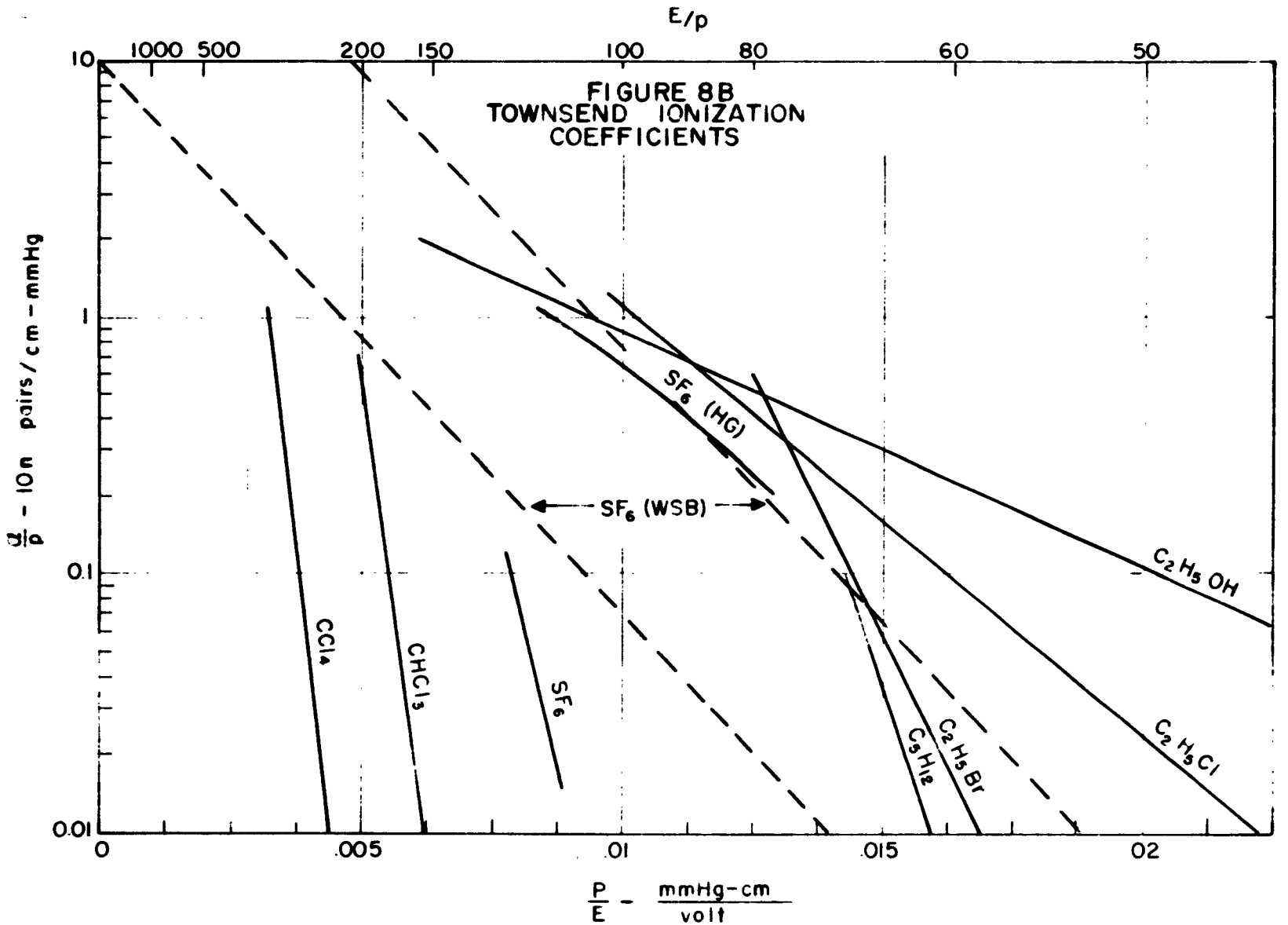

FIGURE 8B
TOWNSEND IONIZATION
COEFFICIENTS

2519-F-88

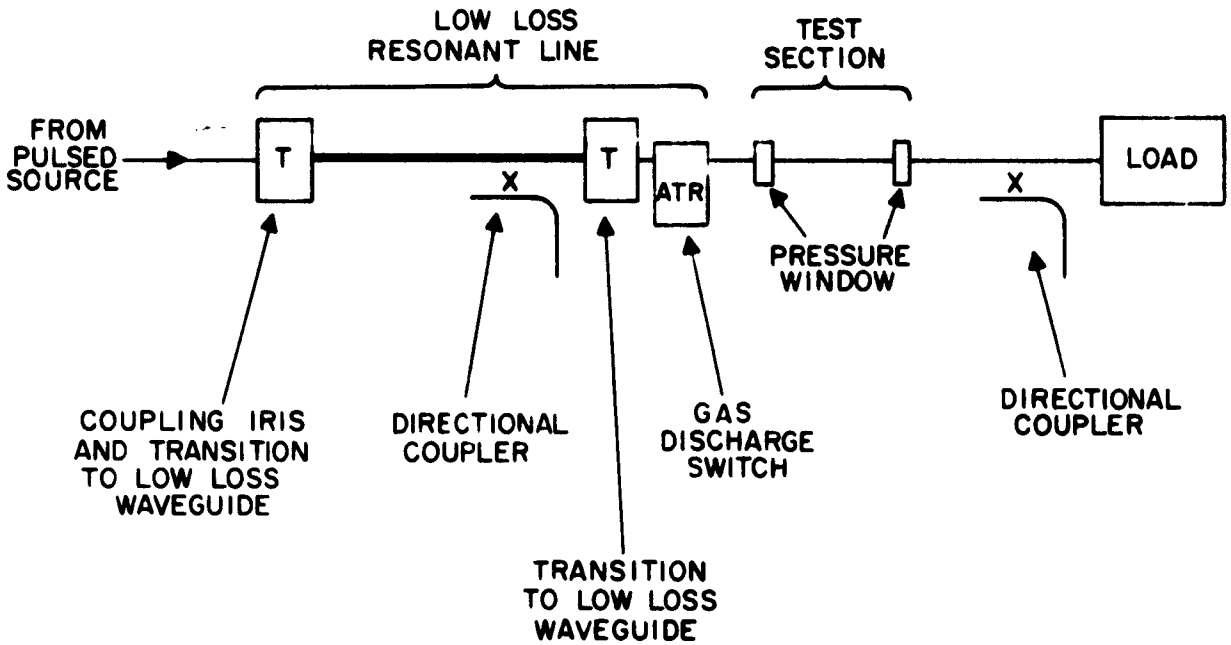

FIGURE 9
SCHEMATIC DIAGRAM OF MICROWAVE NANOSECOND
PULSE GENERATOR

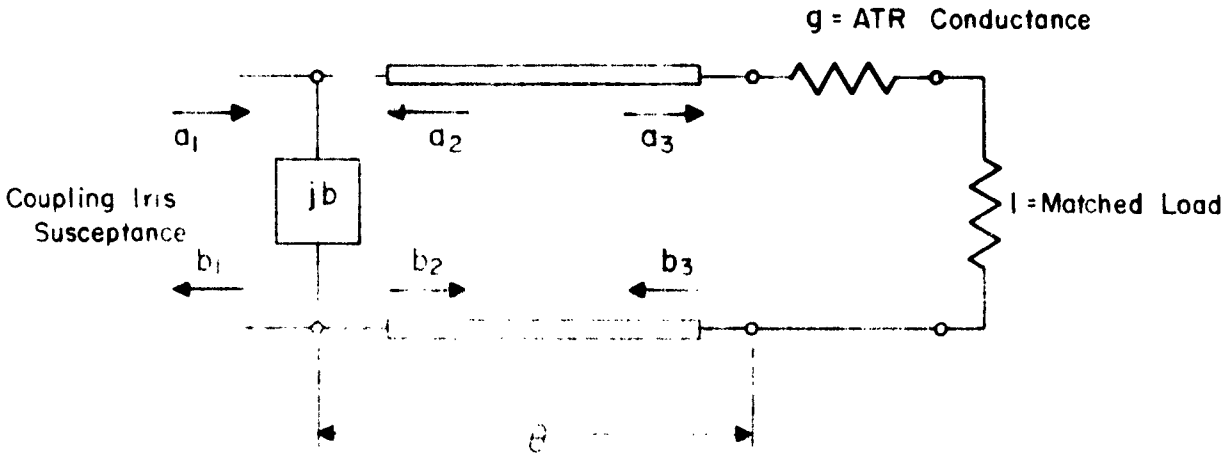

FIGURE 10
CAVITY RESONATOR CIRCUIT

FIGURE 11
EQUIVALENT POWER GAIN IN RESONANT TRANSMISSION LINE VS IRIS COUPLING

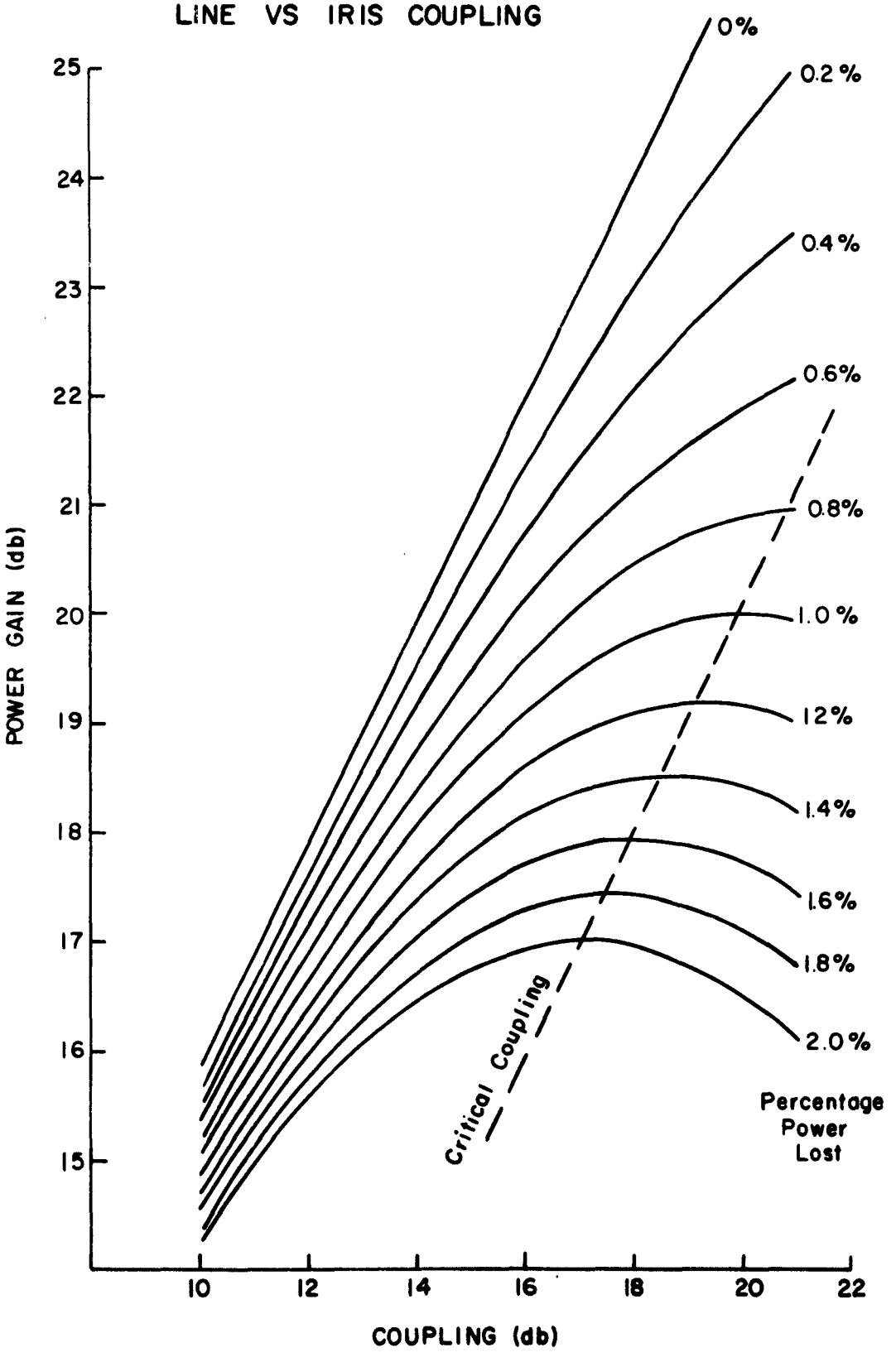

2519-F-11

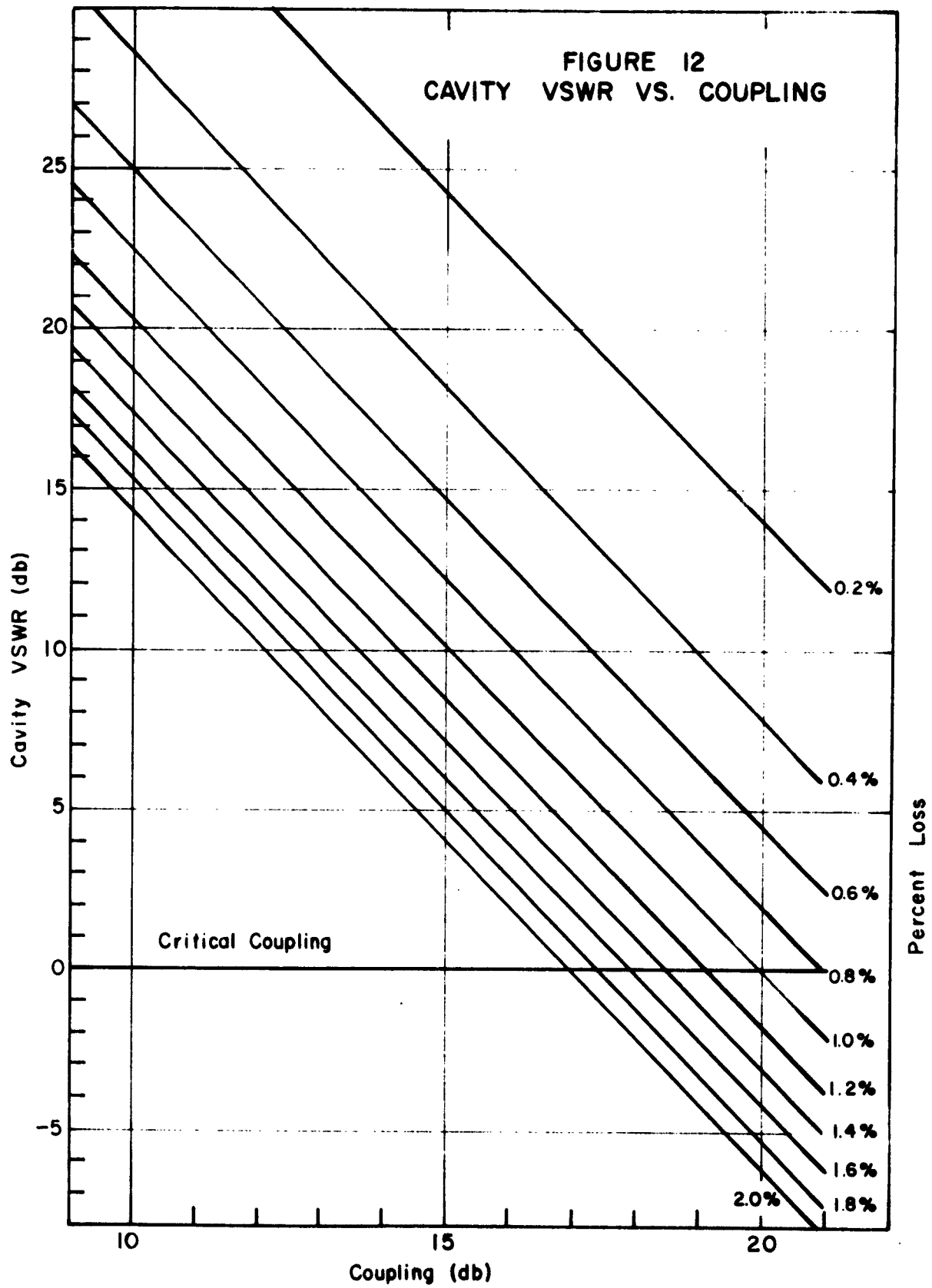
FIGURE 12
CAVITY VSWR VS. COUPLING
25
20
15
10
5
0
-5
Cavity VSWR (db)
Critical Coupling
0.2%
0.4%
0.6%
0.8%
1.0%
1.2%
1.4%
1.6%
1.8%
2.0%
Percent Loss
10
15
20
Coupling (db)

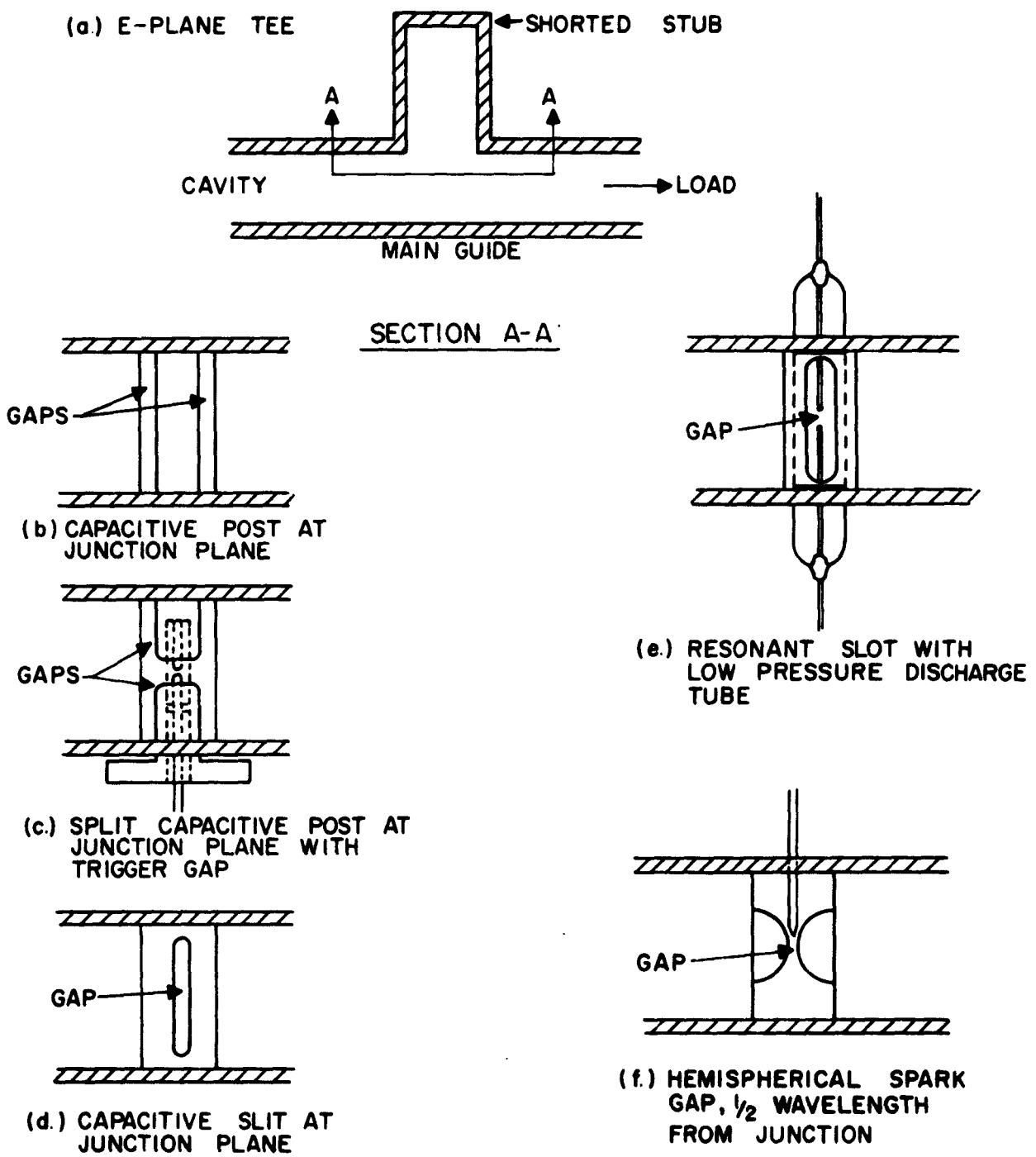

FIGURE 13
SERIES SWITCH FOR THE NANOSECOND PULSE GENERATOR

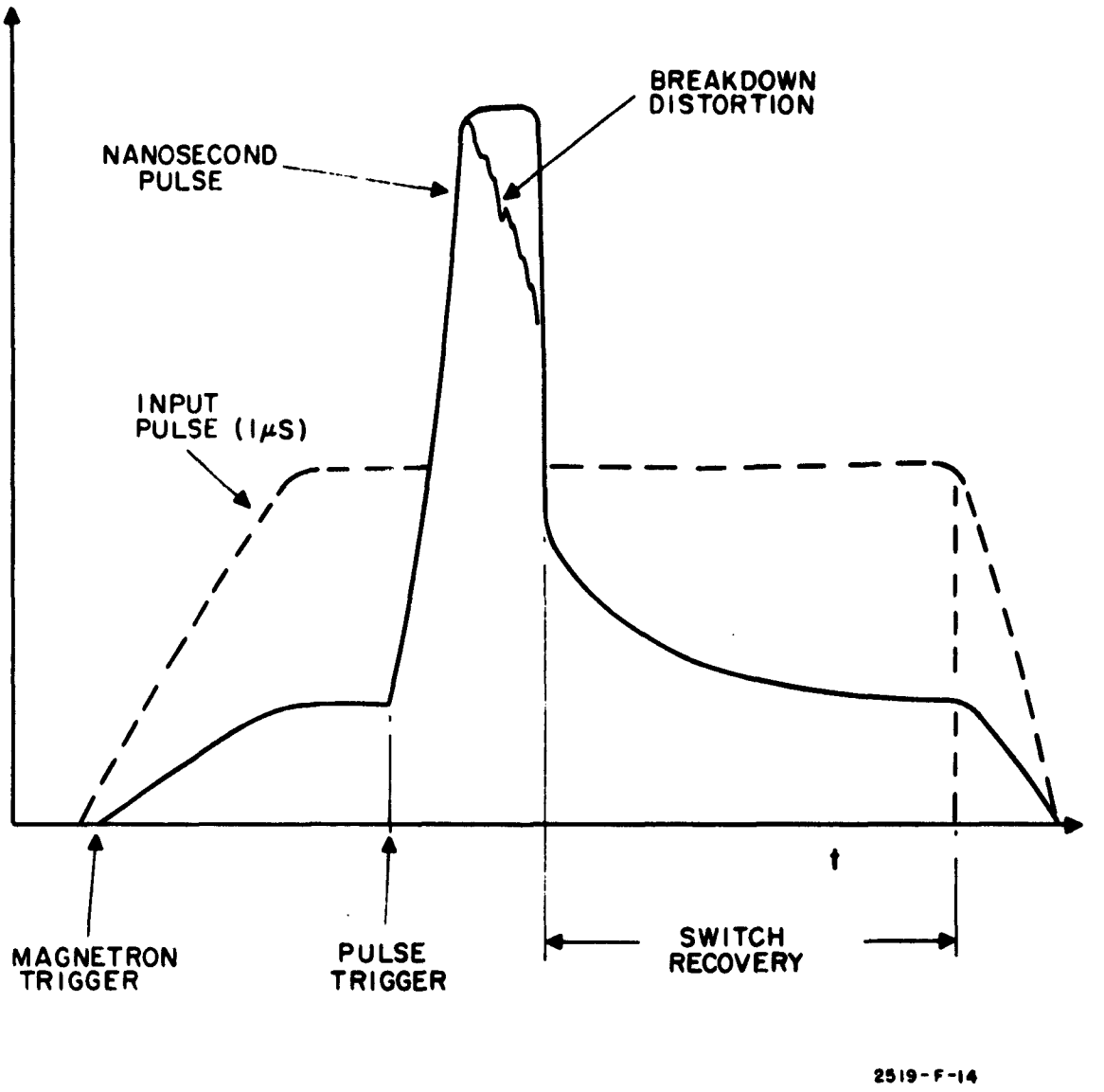

FIGURE 14
WAVEFORMS AT THE BROAD BAND DETECTOR FOR
NANOSECOND BREAKDOWN STUDY

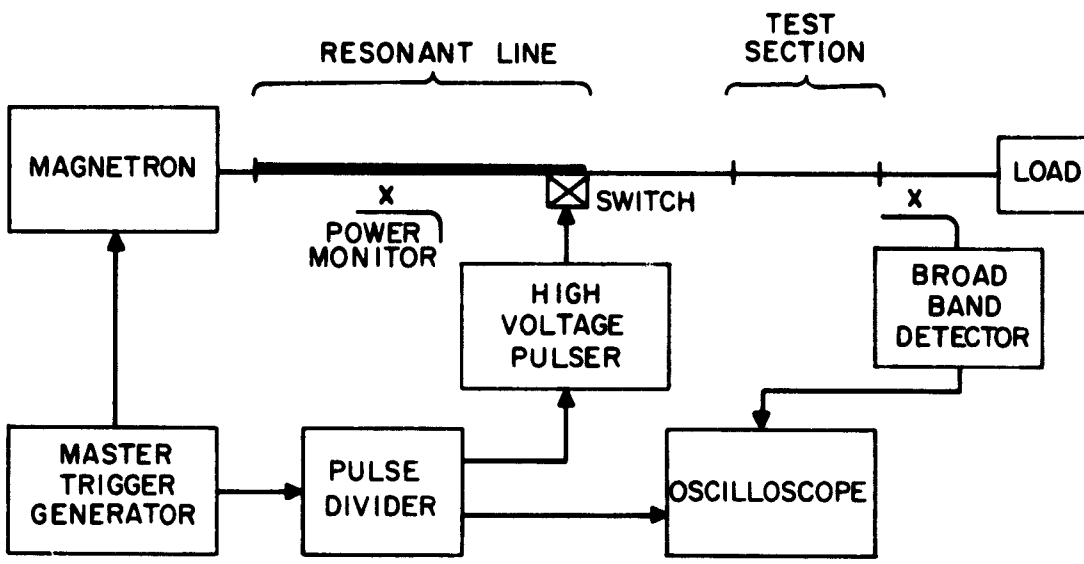

FIGURE 15
BLOCK DIAGRAM OF NANOSECOND BREAKDOWN STUDY INSTRUMENTATION

2519-F-15

Final Report
Contract No. AF30(602)-2782

DISTRIBUTION LIST

	No. of Copies
Rome Air Development Center (RALTP, Attn: W. C. Quinn) Griffiss Air Force Base Rome, New York	3
Rome Air Development Center Attn: RAAPT Griffiss Air Force Base Rome, New York	1
Rome Air Development Center Attn: RAALD Griffiss Air Force Base Rome, New York	1
Rome Air Development Center Attn: GEEIA (ROZMCAT) Griffiss Air Force Base Rome, New York	1
Rome Air Development Center Attn: RAIS, Mr. Malloy Griffiss Air Force Base Rome, New York	1
U. S. Army Electronics R&D Labs. Liaison Officer Rome Air Development Center Griffiss Air Force Base Rome, New York	1
AUL (3T) Maxwell Air Force Base Alabama	1
ASD (ASAPRD) Wright Patterson Air Force Base Dayton, Ohio	1
Chief, Naval Research Lab. Attn: Code 2027 Washington 25, D. C.	1

	No. of Copies
Air Force Field Representative Naval Research Lab. Attn: Code 1010 Washington 25, D. C.	1
Commanding Officer U. S. Army Electronics R& D Labs. Attn: SELRA/SL-ADT Fort Monmouth, New Jersey	1
National Aeronautics & Space Admin. Langley Research Center Langley Station Hampton, Virginia Attn: Librarian	1
RTD (RTGS) Bolling Air Force Base Washington 25, D. C.	1
Central Intelligence Agency Attn: OCR Mail Room 2430 E Street NW Washington 25, D. C.	1
U. S. Strike Command Attn: STRJ5-OR Mac Dill Air Force Base Florida	1
AFSC (SCSE) Andrews Air Force Base Washington 25, D. C.	1
Commanding General U. S. Army Electronics Proving Ground Attn: Technical Documents Library Ft. Huachuca, Arizona	1
ASTIA (TISIA-2) Arlington Hall Station Arlington 12, Virginia	10

	No. of Copies
AFSC (SCFRE) Andrews Air Force Base Washington 25, D. C.	1
Hq. USAF (AFCOA) Washington 25, D. C.	1
AFOSR (SRAS/Dr. G. R. Eber) Holloman Air Force Base New Mexico	1
Office of Chief of Naval Operation (Op-724) Navy Department Washington 25, D. C.	1
Commander U. S. Naval Air Development Center (NADC Lib) Johnsville, Pennsylvania	1
Commander Naval Missile Center Tech. Library (Code No. 3022) Pt. Mugu, California	1
Bureau of Naval Weapons Main Navy Building Washington 25, D. C. Attn: Technical Librarian, DL1-3	1
NAFEC Library Building 3 Atlantic City, New Jersey	1
Redstone Scientific Information Center U. S. Army Missile Command Redstone Arsenal, Alabama	1
Commandant Armed Forces Staff College (Library) Norfolk 11, Virginia	1
ADC (ADOAC-DL) Ent Air Force Base Colorado	1

	No. of Copies
AFFTC (FTOOT) Edwards Air Force Base California	1
Commander U. S. Naval Ordnance Lab (Tech Lib) White Oak, Silver Springs Maryland	1
Commanding General White Sands Missile Range New Mexico Attn: Technical Library	1
Director U. S. Army Engineer R&D Labs. Technical Documents Center Ft. Belvoir, Virginia	1
ESD (ESRL) L. G. Hanscom Field Bedford, Massachusetts	1
Commanding Officer & Director U. S. Navy Electronics Lab (LIB) San Diego 52, California	1
ESD (ESAT) L. G. Hanscom Field Bedford, Massachusetts	1
Commandant U. S. Army War College (Library) Carlisle Barracks, Pennsylvania	1
APGC (PGAPI) Eglin Air Force Base Florida	1
AFSWC (SWOI) Kirtland Air Force Base New Mexico	1
AFMTC (Tech. Library MU-135) Patrick Air Force Base Florida	1

	No. of Copies
Space Sciences, Inc. Attn: Dr. Proud 2 Mercer Road Natick, Massachusetts	1
Braddock, Dunn & McDonald, Inc. Attn: Dr. McDonald Suite 1405 First National Building El Paso, Texas	1